University of Reading

# The EUSTACE project: delivering global, daily information on surface air temperature

Article

Accepted Version

Rayner, N. A., Auchmann, R., Bessembinder, J., Brönnimann, S., Brugnara, Y., Capponi, F., Carrea, L. ORCID: https://orcid.org/0000-0002-3280-2767, Dodd, E. M. A., Ghent, D., Good, E., Høyer, J. L., Kennedy, J. J., Kent, E. C., Killick, R. E., van der Linden, P., Lindgren, F., Madsen, K. S., Merchant, C. J. ORCID: https://orcid.org/0000-0003-4687-9850, Mitchelson, J. R., Morice, C. P., Nielsen-Englyst, P., Ortiz, P. F., Remedios, J. J., van der Schrier, G., Squintu, A. A., Stephens, A., Thorne, P. W., Tonboe, R. T., Trent, T., Veal, K. L., Waterfall, A. M., Winfield, K., Winn, J. and Woolway, R. I. ORCID: https://orcid.org/0000-0003-0498-7968 (2020) The EUSTACE project: delivering global, daily information on surface air temperature. Bulletin of the American Meteorological Society, 101 (11). E1924-E1947. ISSN 1520-0477 doi: 10.1175/BAMS-D-19-0095.1 Available at https://centaur.reading.ac.uk/89293/

It is advisable to refer to the publisher's version if you intend to cite from the work. See Guidance on citing.

To link to this article DOI: http://dx.doi.org/10.1175/BAMS-D-19-0095.1

University of Reading

Publisher: American Meteorological Society

All outputs in CentAUR are protected by Intellectual Property Rights law, including copyright law. Copyright and IPR is retained by the creators or other copyright holders. Terms and conditions for use of this material are defined in the End User Agreement.

www.reading.ac.uk/centaur

**CentAUR**

Central Archive at the University of Reading

Reading's research outputs online

# The EUSTACE project: delivering global, daily information on surface air temperature

Nick A. Rayner

Met Office Hadley Centre, Met Office, FitzRoy Road, Exeter, EX1 3PB

Renate Auchmann

Oeschger Centre for Climate Change Research and Institute of Geography, University of Bern, Bern, Switzerland

Janette Bessembinder

Royal Netherlands Meteorological Institute (KNMI), PO Box 201, 3730 AE De Bilt, The Netherlands

Stefan Brönnimann

Oeschger Centre for Climate Change Research and Institute of Geography, University of Bern, Bern, Switzerland

Yuri Brugnara

Oeschger Centre for Climate Change Research and Institute of Geography, University of Bern, Bern, Switzerland

Francesco Capponi,

Met Office Hadley Centre, Exeter, United Kingdom Now Data Scientist within the Decision Service Team at WorldPay.

Laura Carrea

Department of Meteorology

University of Reading, Reading, RG6 6AL, UK

Emma M. A. Dodd

National Centre for Earth Observation, University of Leicester, Leicester, United Kingdom

Darren Ghent

National Centre for Earth Observation, University of Leicester, Leicester, United Kingdom

Elizabeth Good

Met Office Hadley Centre, Met Office, FitzRoy Road, Exeter, EX1 3PB

Jacob L Høyer

Danish Meteorological Institute, Copenhagen, Denmark

John J Kennedy

Met Office Hadley Centre, Met Office, FitzRoy Road, Exeter, EX1 3PB

Elizabeth C. Kent

National Oceanography Centre, Southampton, UK

Rachel E Killick

Met Office Hadley Centre, Met Office, FitzRoy Road, Exeter, EX1 3PB

Paul van der Linden

Met Office Hadley Centre, Met Office, FitzRoy Road, Exeter, EX1 3PB

Finn Lindgren

University of Edinburgh, School of Mathematics, Edinburgh, United Kingdom

Kristine S. Madsen

Danish Meteorological Institute, Copenhagen, Denmark

Christopher J. Merchant

National Centre for Earth Observation and Department of Meteorology University of Reading, Reading, RG6 6AL, UK

Joel R Mitchelson

Met Office Hadley Centre, Met Office, FitzRoy Road, Exeter, EX1 3PB

Colin P Morice

Met Office Hadley Centre, Met Office, FitzRoy Road, Exeter, EX1 3PB

Pia Nielsen-Englyst

Danish Meteorological Institute, Copenhagen, Denmark

Patricio F. Ortiz

National Centre for Earth Observation, University of Leicester, Leicester, United Kingdom now at Department of Automatic Control and Systems Engineering, The University of Sheffield, Sheffield, United Kingdom

John J Remedios

National Centre for Earth Observation, University of Leicester, Leicester, United Kingdom

Gerard van der Schrier

Royal Netherlands Meteorological Institute (KNMI), PO Box 201, 3730 AE De Bilt, The Netherlands

Antonello A. Squintu

Royal Netherlands Meteorological Institute (KNMI), PO Box 201, 3730 AE De Bilt, The Netherlands

Ag Stephens

Science and Technology Facilities Council, Didcot, United Kingdom

Peter W. Thorne

Department of Geography, National University of Ireland Maynooth, Maynooth, Ireland.

Rasmus T. Tonboe

Danish Meteorological Institute, Copenhagen, Denmark

Tim Trent

National Centre for Earth Observation, University of Leicester, Leicester, United Kingdom

Karen L Veal

National Centre for Earth Observation, University of Leicester, Leicester, United Kingdom

Alison M Waterfall

Science and Technology Facilities Council, Didcot, United Kingdom

Kate Winfield

Science and Technology Facilities Council, Didcot, United Kingdom

Jonathan Winn

Met Office Hadley Centre, Met Office, FitzRoy Road, Exeter, EX1 3PB

R. Iestyn Woolway

Department of Meteorology

115 University of Reading, Reading, RG6 6AL, UK Now at Centre for Freshwater and

116 Environmental Studies Dundalk Institute of Technology, Dundalk, A91 K584, Ireland

117

118 Corresponding author: Nick A. Rayner, nick.rayner@metoffice.gov.uk

119

120 Capsule

121

122 The main goals and activities of the EUSTACE project are discussed along with some key

123 results, including a global, multi-decadal daily air temperature record from satellite and *in*

124 *situ* measurements.

Abstract

Day-to-day variations in surface air temperature affect society in many ways, but daily surface air temperature measurements are not available everywhere. Therefore, a global daily picture cannot be achieved with measurements made *in situ* alone and needs to incorporate estimates from satellite retrievals.

This article presents the science developed in the EU Horizon 2020-funded EUSTACE project (2015-2019, https://www.eustaceproject.org) to produce global and European, multi-decadal ensembles of daily analyses of surface air temperature complementary to those from dynamical reanalyses, integrating different ground-based and satellite-borne data types. Relationships between surface air temperature measurements and satellite-based estimates of surface skin temperature over all surfaces of Earth (land, ocean, ice and lakes) are quantified. Information contained in the satellite retrievals then helps to estimate air temperature and create global fields in the past, using statistical models of how surface air temperature varies in a connected way from place to place; this needs efficient statistical analysis methods to cope with the considerable data volumes. Daily fields are presented as ensembles to enable propagation of uncertainties through applications. Estimated temperatures and their uncertainties are evaluated against independent measurements and other surface temperature data sets.

Achievements in the EUSTACE project have also included fundamental preparatory work useful to others, for example: gathering user requirements; identifying inhomogeneities in daily surface air temperature measurement series from weather stations; carefully quantifying uncertainties in satellite skin and air temperature estimates; exploring the

interaction between air temperature and lakes; developing statistical models relevant to non-Gaussian variables; and methods for efficient computation.

150 Body text

151 EU Surface Temperature for All Corners of Earth (EUSTACE,
152 https://www.eustaceproject.org) is a 4-yr research project funded by the European Union
153 Horizon 2020 research and innovation programme (EU H2020; Grant Agreement 640171;
154 see Appendix A for a list of the Consortium's institutions) that started on 1 January 2015.
155 EUSTACE has used temperature estimates from satellites to boost the amount of
156 information available beyond that provided by weather stations and ships to help to
157 construct a prototype global, multi-decadal daily air temperature record presented on a
158 0.25° latitude by 0.25° longitude grid.

159

160 Near-surface air temperature (typically measured at a height of about 2 m above ground
161 level at meteorological stations) is a fundamental quantity for many of the activities
162 undertaken in climate science and in many of the societal concerns that climate services aim
163 to support; it is something that we all experience directly in our day-to-day lives. Near-
164 surface air temperature has been measured almost continuously in some places and across
165 the global oceans by ships for well over a century. Designated as an Essential Climate
166 Variable (ECV), these records allow for the construction of a useful climate data record
167 (CDR) in those places for the period covered. Globally, however, there a number of locations
168 where either access to the measurements is not possible, or no air temperature records
169 exist. As well as long records of direct measurements of near-surface air temperature, we
170 have information from satellite retrievals (i.e. remotely-sensed, indirect estimates) of
171 temperature. However, satellite retrievals tend not to pertain to the air temperature that
172 we experience directly, but either to an average temperature of a higher layer in the

atmosphere or to the skin temperature of the surface of the Earth. These quantities are related to near-surface air temperature, more or less tightly depending on the type of surface and the surface-lower-atmosphere interactions. Therefore, it is possible to use satellite-derived temperatures together with near-surface air temperature measurements to create a more complete climate data record of air temperature. Thus, EUSTACE created a prototype global climate data record of near-surface air temperature for every day since January 1850 using both direct measurements of air temperature and estimates of it based on satellite skin temperature retrievals.

Near-surface air temperature products provide valuable information for a range of activities, from the monitoring of current conditions (e.g. Sánchez-Lugo et al. 2019) to the assessment of past variability (e.g. Osborn et al. 2017) to their use in seasonal-to-decadal forecasting (e.g. Kushnir et al. 2019), climate model evaluation (e.g. Walters et al. 2019), detection and attribution of climate change (e.g. Jones and Kennedy 2017), Intergovernmental Panel on Climate Change Assessments (e.g. Hartmann et al. 2013), agricultural modelling (e.g. Weedon et al. 2011), health modelling (e.g. Xu et al. 2019) and other downstream uses. Such a daily surface air temperature product could form part of the future operational monitoring system for surface air temperature over the polar regions, over Africa and South America. EUSTACE has already enabled monitoring of lake surface water temperature to be included in the annual State of the Global Climate reports (for the years 2015, 2016, 2017 and 2018; Woolway et al., 2016, 2017a and 2018; Carrea et al., 2019). EUSTACE products are complementary to products from dynamical reanalyses (e.g. Buizza et al. (2018)) with much of the work dedicated to the preparation of input surface temperature observations, for

196 which EUSTACE has performed thorough uncertainty analyses, which were previously
197 lacking.

198

199 Dynamical reanalyses combine historical and recent observations with numerical weather
200 prediction models to produce dynamically-consistent reconstructions of past weather and
201 climate. These reanalyses require observational data with well-characterised uncertainties.
202 The new, validated, estimates of uncertainty in satellite surface skin temperature
203 observations developed by EUSTACE are of benefit to them. EUSTACE products also provide
204 an alternative source of near-surface air temperature data that is independent from
205 numerical weather prediction models and extends further back in time than most dynamical
206 reanalyses.

207

208 Results from scientific projects are often not produced in a format that can be used easily by
209 others; in general, processing or translation is needed. Two-way interaction with potential
210 users from the start of a project helps to increase the relevance and usability of products to
211 various potential user groups. EUSTACE collected information on user requirements in several
212 ways, via: user consultation workshops; questionnaires and interviews; a literature review on
213 user requirements (Bessembinder et al. 2016; Bessembinder 2017, including the results from
214 a large number of national and EU projects); testing of example mock-up datasets; and
215 describing specific use cases with “trail blazer” users.

216

These activities resulted in greater insight into how climate data are used, data format preferences, and which variables are needed (i.e. not just daily mean temperature, but also minimum and maximum temperature), amongst other things. We used many of the user requirements collected to design the EUSTACE data file structure and the user guides; for example, a quick start guide is provided as part of the product user guide, together with example use cases.

While many of the ideas used within EUSTACE have been trialled elsewhere for individual regions (e.g. Cristóbal et al. (2008)), or for different time scales (e.g. Kilibarda et al. (2014)), EUSTACE has brought them together for the first time to create global, multi-decadal daily products. EUSTACE has performed an integrating function, bringing together products and expertise from a wide range of European, national and international initiatives. EUSTACE has also followed much of the road map of "recommended steps towards meeting societal needs for surface temperature understanding and information" set out previously in the EarthTemp Network Community Paper (Merchant et al. 2013). In particular, EUSTACE has made progress in seven out of the ten broad aims identified therein:

- develop more integrated, collaborative approaches to observing and understanding Earth's various surface temperatures;
- build understanding of the relationships between different surface temperatures, where presently inadequate;
- make surface temperature datasets easier to obtain and exploit for a wider constituency of users;

- consistently provide realistic uncertainty information with surface temperature datasets;
- communicate differences and complementarities of different types of surface temperature datasets in readily understood terms;
- rescue, curate and make available valuable surface temperature data that are presently inaccessible; and
- build capacities to accelerate progress in the accuracy and usability of surface temperature datasets.

Computer code has been developed both to estimate air temperature from satellite data and to create daily maps of mean air temperature; this code has been publicly released (Rayner 2019). Information contained in the satellite retrievals helps to create more-complete fields in the past, via statistical models of how surface air temperature varies in a connected way from place to place. As the data volumes involved are considerable, the EUSTACE partnership included statisticians and computer scientists, enabling the development of efficient analysis methods. As a result, EUSTACE has been able to demonstrate that these methods can be built into a fully functional processing system, with research-level maturity (EUMETSAT, 2014) which exploits the features of modern high performance computing resources to deliver the more-complete datasets described below. This system could be used in future to update some of the EUSTACE data sets described here to enable their use in climate monitoring.

261 The datasets that are currently commonly used to monitor surface temperatures globally
262 are constructed as a combination of air temperature observations over land and sea surface
263 temperature observations over ocean. The current versions of the most widely used global
264 near-surface temperature datasets, HadCRUT4 (Morice et al., 2012), NOAAGlobalTemp
265 (Smith et al., 2008; Vose et al., 2012) and GISTEMP (Hansen, 2010), extend from the mid-
266 19th century to present and are derived from *in situ* observations only; temperature
267 retrievals from satellites are not used in their construction. These global temperature
268 datasets are presented at monthly resolution because summaries of monthly average
269 temperatures are more commonly available for individual meteorological stations and cover
270 a greater region of the Earth than daily or sub-daily summaries in the 19th century and early
271 20th century. The density distribution of available *in situ* temperature observations limits
272 the spatial resolution of these products. For example, HadCRUT4 is provided as monthly
273 fields on an equi-angle latitude-longitude grid at $5^{o}$ resolution.

274

275 Surface air temperature datasets covering land regions, but not ocean or sea ice, are
276 available at higher spatial and temporal resolutions. For example, Rhode (2013a; 2013b) use
277 a larger number of meteorological stations than do HadCRUT4, NOAAGlobalTemp or
278 GISTEMP, together with a statistical interpolation algorithm, to produce a monthly surface
279 air temperature dataset at higher spatial resolution; an experimental daily analysis has also
280 been produced. Other high-resolution datasets of air temperatures over land are available
281 and are commonly used in climate modelling (Harris et al., 2013) and hydrological modelling
282 (Weedon et al., 2011). Higher temporal resolution air temperatures derived from land
283 meteorological station observations are also available, including the daily GHCN-D databank

(Menne et al., 2012), and the sub-daily HadISD databank (Dunn et al., 2016). Gridded temperature fields based on GHCN-D are available in the HadGHCN-D dataset (Caesar, et al., 2006) covering a time period from 1950 to present. HadISD is presented as time series for individual meteorological stations only. However, none of these latter datasets are based on homogenised data (see below).

The existing coarse-resolution global temperature datasets are widely used in global and regional climate assessments; however their utility is limited in some applications that require information at high temporal and/or spatial resolutions, such as the assessment of temperature extremes, national climate assessments, regional impact studies and validation of climate simulations from high-resolution climate models. These global temperature datasets are also often expressed in terms of temperature anomalies (temperatures relative to average conditions over some reference period), rather than in terms of absolute temperature information, which is commonly needed in these applications. EUSTACE provides products that can be used for the study of absolute temperatures, as well as providing information relevant to temperature anomalies.

Figure 1 provides an overview of the EUSTACE process and shows how different activities linked together to transform the source datasets (Appendix B) into the series of EUSTACE products (Appendix C). Source data sets were chosen to maximise our opportunity to quantify the components of uncertainty (in the case of satellite data) and the amount of historical daily information (in the case of weather station data). Wrapped around these scientific developments were interactions throughout the project with potential users.

Evaluation against independent reference measurements (Veal, 2019a) and comparison with other related products (Veal, 2019b) put EUSTACE work into context.

Through this development process, EUSTACE has contributed to advancing and enabling climate science in five main areas:

1) Detecting and correcting for non-climatic discontinuities in weather station series: to provide an accurate picture of variations in air temperature, measurements at weather stations have been checked for any jumps in the series and then corrected (Squintu et al., 2019a and b). Such discontinuities might have arisen from changes in the surroundings of the weather station, the instruments used, the location of the station, or the measurement procedure (Brugnara et al., 2019).
2) Estimating consistent skin temperature uncertainties: EUSTACE used satellite data on the surface skin temperature of the land, ocean and ice, obtained from European reprocessing projects with diverse approaches to estimating uncertainty. Therefore, we derived consistent uncertainty estimates for these data over all surfaces in order to use them together effectively (Ghent et al. 2019; Nielsen-Englyst et al. 2019a).
3) Estimating air temperature from satellite data: while in some locations air temperature records can span periods of a century or more, in many areas there is a lack of information. EUSTACE has helped to provide daily air temperature information by using temperature estimates from satellite measurements to boost the amount of information beyond that already available from weather station records and ships (Nielsen-Englyst et al. 2019; Høyer et al. 2018; Kennedy and Kent, 2019).

4) Understanding the role of lakes: a number of EUSTACE studies explored various aspects of the relationship between lake surface water temperature and air temperature, demonstrating the place of lakes in the global climate system, their response to climate change and the importance of using spatially-resolved data to explore aspects of the response of lakes to climate change (Woolway and Merchant, 2017; 2018; Woolway et al. 2017b, c, d; 2018b).
5) Estimating complete fields: EUSTACE used cutting-edge statistical methods to exploit the links between air temperature in different places and through time to estimate daily air temperatures in places and at times when neither direct measurements, nor estimates from satellite were available

Hereafter, we will briefly discuss these activities, together with the independent validation of EUSTACE products.

**Detecting and correcting for non-climatic discontinuities in weather station series**

Most instrumental temperature series suffer from non-climatic artefacts (i.e. discontinuities or "breaks"; e.g., due to the relocation of weather stations, changes in the instrument shelter, changes in observation practices) which often result in sudden changes in the time series (e.g. Peterson et al., 1998; Brandsma and Können, 2006). Changes like this are not often adequately documented, so we need to use an automated method to detect them that we can apply to a global dataset. Correcting for these changes is termed

352 "homogenisation". Until recently, homogenisation efforts have mostly addressed the
353 monthly or annual time scales and have only adjusted shifts in the mean value. This is not
354 sufficient when dealing with daily data as inhomogeneities can affect not just the mean, but
355 the entire distribution of variables (Trewin, 2013). The effects of, for example, shelter
356 changes on temperature depend non-linearly on the ambient weather conditions such as
357 sunshine and wind.

358

359 Homogenisation of daily and sub-daily data has received more attention in recent years (e.g.
360 Aguilar et al. 2008), but efforts are still rare compared to work on monthly data (Venema et
361 al. 2012). Existing methods correcting daily or sub-daily temperature data can be grouped
362 into three basic categories:

363 1) Corrections of the mean: Methods that start from monthly mean break sizes (i.e.
364 sizes of non-climatic discontinuities), which are then distributed to individual days.
365 Daily corrections are computed by fitting a spline or piecewise linear function
366 between monthly mean corrections (e.g. Vincent et al. 2002). This is the easiest
367 approach, but comes with a risk that the tails of the distribution would not be
368 properly corrected.
369 2) Corrections of higher order moments of the distribution: Methods that directly
370 adjust the distribution of daily temperature based on a daily reference series (e.g.
371 Trewin, 2013). This is better suited for extremes, but it requires longer and better
372 correlated reference series than method 1).

3) Methods that incorporate basic physics such as the effects of radiation and ventilation on the temperature shield (e.g., Auchmann and Brönnimann 2012). This requires detailed metadata that are not usually available for large datasets.

Until quite recently, no global dataset of homogenised daily land surface air temperature was available. Corresponding homogenisation work was restricted to a few regions such as Canada (Vincent et al. 2002), the Mediterranean region (e.g., Brunet et al. 2006, Kuglitsch et al. 2009), Australia (Trewin, 2013) and China (Xu et al. 2013).

Most break-detection methods require highly correlated reference series. However, a non-climatic network-wide break point (e.g., the simultaneous introduction of new instruments) can be difficult to detect if reference series are from the same network. For global studies, only unhomogenised daily temperature data have been available through GHCN-Daily and other sources, which are not suitable in all locations for analysing trends in extremes, for example. Berkeley Earth have produced an experimental gridded daily temperature product over land (see a description of their method in Rohde et al. (2013a; b)), but their homogenised daily station series are not available and the analysis was constructed without directly homogenising daily data. Rather, Rohde et al. (2013 a; b) constructed fields of daily anomalies (from their monthly mean values) and added them to the existing homogenised monthly dataset.

EUSTACE has combined multiple break-detection algorithms (those of Caussinus and Mestre (2004), Toreti et al. (2012), and Wang (2008)). We applied them either to annual and semi-

395 annual averages of differences between each station and neighboring reference series (our
396 relative tests; all methods used), or to the averages of the target station alone (our absolute
397 test; Wang (2008) only used), in the absence of neighboring stations or if available reference
398 series are not suitable (Brugnara et al. (2019) provides details). Using multiple methods of
399 detecting discontinuities provides an ability to assess the robustness of the results. Figure 2
400 illustrates the coverage of the EUSTACE station dataset and indicates the type of break
401 detection method applied to each station (relative or absolute) and also where application
402 of the break detection methods has not been possible because of insufficient record length
403 (i.e., less than 10 years). A simple likelihood index is formed from a 50-member break
404 detection ensemble and users of the EUSTACE global station dataset can select a likelihood
405 threshold appropriate to their needs, such that the detection power is maximised whilst
406 minimising the false alarm rate. This is the first global daily station dataset with estimated
407 locations of non-climatic discontinuities and their likelihood, together with valuable
408 metadata, e.g. on resolution of measurements.

409

410 In addition to break detection, the EUSTACE global station dataset has undergone other
411 quality checks both on the air temperature measurements themselves and on reported
412 station altitudes (Brugnara et al. 2019). Appendix C provides a link to the resulting dataset of
413 daily mean, maximum and minimum temperature.

414

415 For European weather station series, EUSTACE has made adjustments, where possible, to
416 reduce the impact of non-climatic discontinuities. Briefly, we used an iterated quantile-
417 matching approach (an example of method type 2 above) to adjust the distributions of the

418 measurements, not just their means, by comparing to the measurement distributions at
419 nearby reference stations (Squintu et al. (2019a; b) give details). The homogenisation brings
420 the distributions before and after each station change much closer together, adjusting for
421 the non-climatic effects of such discontinuities.

422

423 Applying the quantile matching to the whole European station dataset has an impact on the
424 apparent trends in temperature over Europe (see Squintu et al., 2019a). Sometimes, the
425 EUSTACE corrections increase the trend and sometimes they decrease it. Where stations
426 previously showed negative trends since 1951, they show positive trends in most cases after
427 homogenisation; in all cases making them more consistent with their neighbouring stations.

428

429 This is the first time that a pan-European station dataset of daily data has been
430 homogenised to reduce the impact of non-climatic discontinuities. The homogenised
431 European station dataset is provided separately from the global station dataset and
432 comprises part of the European Climate Assessment and Dataset (ECA&D) product. A
433 gridded 100-member ensemble dataset available either on a $0.1^{o}$ latitude by $0.1^{o}$ longitude
434 grid or a $0.25^{o}$ latitude by $0.25^{o}$ longitude grid, based on the homogenised station records
435 has also been developed as a contribution to the next version of the E-OBS dataset (Cornes
436 et al., 2018). A two-step method (documented in Cornes et al., 2018) was used to create the
437 ensemble: (i) the daily values were fitted with a Generalised Additive Model, to capture
438 large-scale spatial trends and (ii) the residuals from this were then interpolated using
439 stochastic Gaussian Random Field simulation. Appendix C provides a link to the CEDA
440 catalogue record for these datasets of daily mean, maximum and minimum temperature.

441

442 **Estimating consistent skin temperature uncertainties**

443

444 EUSTACE uses surface temperature retrievals over land, ocean and ice based on information
445 gathered by infra-red satellite sensors. One of our key aims is to estimate the uncertainty in
446 our air temperature products, so first we addressed the inconsistency in the availability of
447 uncertainty estimates for skin temperature retrievals over different surfaces. Here skin
448 temperature is the temperature at a few microns below the top-most surface of the land,
449 ocean or ice.

450

451 Uncertainty in surface skin temperature retrieved from satellites arises from various sources
452 (Merchant et al., 2015):

453 1) Radiometric noise in the measurements made by the satellite sensor. This is usually
454 the simplest component of uncertainty, and a standard "uncertainty propagation"
455 can be applied to derive the surface skin temperature uncertainty associated with
456 any surface skin temperature retrieval, given information about the radiometric
457 noise. There is usually no or negligible correlation of error from this source between
458 different surface skin temperature retrievals.
459 2) Limitations of the retrieval process would introduce uncertainty into the surface skin
460 temperature even if the actual radiometric measurements made had zero error. For
461 physically-derived retrievals, this component can be isolated and estimated if
462 representative simulations of the retrieval process are available; this is not the case

where purely empirical relationships are used. An important aspect of this component of uncertainty is that the errors are likely to be correlated in space and time, and therefore may not "average out" in a simple way when transforming data from finer to coarser spatio-temporal scales.

3) Effects that are more systematic, principally: sensor calibration (which may drift over time) and radiative transfer simulation (including the effects of imperfect instrument characterisation and incorrect surface emissivity assumptions, although sub-pixel emissivity variability over land is usually considered random despite having local, coherent structure. See Ghent et al. 2019 for further discussion of uncertainties arising from misspecification of emissivity).

In addition to the above, error is introduced into surface skin temperature estimates because of imperfect cloud detection (when infrared sensors are used, as in EUSTACE; see Bulgin et al. 2018), unrecognised atmospheric aerosol, sensor anomalies, signal contamination, geo-location error, corrupted data streams, etc. Errors arising from these contributing sources are often far from Gaussian in their distributions, with complex effects on surface skin temperature uncertainty. These uncertainties have not been quantified in EUSTACE.

For all surfaces, EUSTACE estimated uncertainties partitioned according to the correlation structure of the different contributing error sources, following the method developed by Merchant et al. (2014) and expanded in Merchant et al (2015). Uncertainties are split into those arising from uncorrelated random effects, from effects which are locally correlated

(these arise from atmospheric effects and/or from uncertainties in the specification of emissivity) and from effects which are correlated over large space and time scales. The derivation of uncertainties in land surface temperature is documented in Ghent et al. (2019) and in Nielsen-Englyst et al. (2019a) for ice surface temperature. Uncertainties in sea surface temperature are as calculated by Merchant et al. (2014).

Links to EUSTACE products containing these consistently-estimated uncertainties are given in Appendix C.

**Estimating air temperature from satellite skin temperature**

Before we can use the satellite data to estimate air temperature, we have to understand the relationship between surface air temperature and surface skin temperature and how it varies throughout the day, by surface type and through the seasons. The challenges are different in each domain, so EUSTACE explored the relationship separately over land, ocean and ice. Based on our understanding of the factors influencing the relationship in each case, we developed multiple linear regression relationships. As well as *in situ* measurements and satellite skin temperature estimates, these use extra information to help to categorise the way the skin/air temperature relationship behaves, such as vegetation, latitude and snow cover. Inclusion of altitude was found to provide no additional skill due to a lack of high altitude weather stations, although it does affect the relationship. Wind speed has a clear influence on the relationship (Good 2016), but use of wind speed information (from a

dynamical reanalysis) in the regression provided no additional skill. The changing vegetation fraction information used also acts as a proxy for some other relevant surface effects, such as urbanisation, but there was no explicit attempt here to model the impact of urbanisation. The uncertainty arising from excluded effects is also not dealt with explicitly in the error model. We withheld a pre-defined set of *in situ* measurements from the regression to use in validation of the results. We then used the regression relationships to estimate air temperature when and wherever a satellite skin temperature retrieval is available, i.e. in clear-sky conditions over the period of record.

The relationship between skin and air temperature is not straightforward; Good (2016) explores this over land. Simultaneously-measured air and skin temperature vary relative to each other over the course of a day. Depending on conditions, the skin temperature can become much warmer than the air temperature when the sky is clear, but when cloud is present, the skin temperature quickly decreases to a value close to the air temperature. The daily maxima and minima in the skin and air temperatures usually occur at different times of day and the amplitudes of their diurnal cycles are often quite different. These differences also vary with season and with location. Nielsen-Englyst et al. (2019b) found a very different relationship over ice-covered surfaces in Greenland with the closest coupling between skin and air temperature occurring at noon in the summer under clear skies, when the sun warms the surface. At other times, particularly in darkness, the surface is often colder than the air above it through radiative cooling and the formation of a surface inversion layer. Under overcast skies, the surface can become warmer than the overlying air during more of the day. Spatial mismatches between satellite retrievals and *in situ* measurements mean

that care needs to be taken on the resolution of satellite data used to develop the relationships. Consequently, we train our regression over land on skin temperature at 0.05° latitude by 0.05° longitude resolution, as the relationship with air temperature has been shown to peak at this resolution (Sohrabinia et al. 2014). Weather stations were preferentially selected for model training if their land cover type matched the dominant land cover type in the surrounding 5° latitude by longitude area. Retrievals from infrared sensors are only available in clear sky conditions, so we might expect that to bias our understanding of the relationship. By using *in situ* measurements from both clear and cloudy conditions, we mitigate the impact of this (see Høyer et al. 2015; Nielsen-Englyst et al., 2019a; Kennedy and Kent, 2019 for details on the relationships between skin and air temperature across different surfaces).

Once a regression relationship has been derived, that relationship is used to estimate air temperature where we have skin temperature retrievals. We perform this procedure separately over land, ocean and ice and build up a global picture of air temperature based on the available satellite measurements (see an example in Figure 3). Global regression coefficients are used over land. Here, the estimation is most challenging, largely due to a lack of representative station measurements, in high altitude regions (for both daily minimum and maximum temperature) and at high latitudes and/or with high snow cover (for daily maximum).

Since we previously estimated our skin temperature retrieval uncertainties arising from components with different correlation structures, when we propagate those through the

554 regression-based air temperature estimation together with the uncertainties inherent in the
555 estimation, we can also derive components of uncertainty in the air temperature estimates
556 arising from random, locally-correlated and systematic effects. This means that the
557 uncertainties in our air temperature estimates are also estimated consistently across the
558 different surfaces and can be propagated appropriately through an application.

559

560 EUSTACE air temperature estimates from satellite are provided on a 0.25° latitude by 0.25°
561 longitude grid in separate files for each surface (land, ocean and ice). Daily mean
562 temperatures are provided over ocean and ice and daily maximum and minimum is
563 provided over land. Appendix C provides access information.

564

565 **Understanding the role of lakes**

566

567 EUSTACE has undertaken work using both lake surface water temperature from satellites
568 and from *in situ* measurements gathered by the project to better understand the
569 relationship between lake surface water temperature and near surface air temperature.

570

571 Lakes can show an amplified response of summer surface water temperature to near surface
572 air temperature variability over the lake. This amplification of response is variable, but greater
573 for cold lakes (e.g., those situated at high latitude and high elevation) and for deep lakes
574 (Woolway and Merchant, 2017). Over-lake atmospheric boundary-layer stability is found to
575 be more frequently unstable, with over-lake air temperature lower than lake surface water

576 temperature, at lower latitudes (Woolway et al., 2017b). In summer, the frequency of
577 unstable conditions decreases with increasing lake area, as a result of an increase in wind
578 speed with lake size, affecting heat and carbon fluxes between the atmosphere and the lake.
579 A study of Central European lakes shows variable warming rates across the year, but these
580 lakes have warmed most in spring with significant trends seen over the last few decades
581 (Woolway et al., 2017c). Abrupt changes seen in these lakes in the 1980s are consistent with
582 abrupt changes in air temperature at the same time. Warming trends seen across nineteen
583 large Northern Hemisphere lakes (Woolway and Merchant, 2018) vary significantly across
584 lakes as well as between them. Deeper areas of large lakes exhibit longer correlation time
585 scales of lake surface water temperature anomalies and a shorter stratified warming season.
586 Deep areas of large lakes consequently display higher rates of increase of summer lake surface
587 water temperature.

588

589 Wind speed has a substantial impact on stratification of lakes, which can have a greater
590 influence than air temperature (Woolway et al. 2017d), and is a controlling factor on lake-air
591 turbulent heat fluxes. Variations in turbulent heat fluxes over lakes have a marked seasonal
592 cycle in some cases, with heat loss higher over large lakes and at low latitudes (Woolway et
593 al., 2018b). The relative contribution of latent and sensible heat fluxes to the total heat flux
594 differs between lakes and with latitude.

595

596 The relationship between lake surface water temperature and near surface air temperature
597 is a two-way interaction. Air temperature influences lake temperature (via its role in
598 turbulent fluxes) and the presence of a lake has an impact on the air temperature in its

vicinity; an impact that metaphorically has some "memory" of earlier air temperature anomalies by virtue of the thermal inertia of the lake. The lake influence can be substantial, and in some instances be in excess of 2°C. In some regions, in particular where lakes are abundant (e.g., Northern Europe), their influence on the surrounding climate needs to be considered. For EUSTACE, the key question is how the lake modifies the dynamics over time of the daily minimum, maximum, and mean air temperature in its vicinity. EUSTACE has estimated the region of influence of lakes globally, provided in the Supplemental material to facilitate the inclusion of this effect in future air temperature analyses.

**Estimating more-complete fields**

Having used surface skin temperature retrievals over all surfaces of Earth to estimate near surface air temperature, we have global, but not globally-complete, fields covering the last few decades. Gaps remain due to the impact of clouds on the satellite estimates, for example. We also have over a century and a half of spatially-incomplete data from ships and weather stations. Night-only ship data were used, to avoid daytime biases, and adjusted to represent air temperature at 2 m following Kent et al., 2013. To try to complete the picture, we needed to use statistical modelling to capture information on how temperature covaries between locations. This information is contained in both the satellite estimates from the recent past and the weather station and ship measurements (Woodruff et al. 2011). The statistical modelling helps us understand unobserved regions on any given day.

621 The state-of-the-art in the spatial statistics research community was previously far ahead of
622 the methods that had been introduced to the Earth sciences, both in terms of generality and
623 computational efficiency. In particular, methods capable of propagating uncertainty from
624 multiple input data sources and realistic modelling of uncertainty due to spatial variability
625 had seen only very limited use in the Earth sciences.

626

627 Current methods for spatial interpolation in Earth sciences that also include statistical
628 uncertainty estimates fall mainly into two categories: low-dimensional function
629 representations (e.g. Banerjee et al., 2008, Wikle, 2010), and local covariance-based kriging
630 methods (e.g. Furrer et al., 2006). Given a realistic computational effort, none of these
631 approaches provide full quantification of uncertainties on long and short spatial and
632 temporal scales simultaneously; low-dimensional basis methods cannot capture small-scale
633 variability and dealing with statistical non-stationarity is challenging for covariance-based
634 methods. New techniques for statistical spatio-temporal models have been developed
635 recently by combining numerical methods for stochastic partial differential equations
636 (SPDEs) with efficient Bayesian computations for Markov random fields. When combined
637 with methods for fast computations for hierarchical statistical models (e.g., Rue et al., 2013)
638 they can handle multiple scales as well as non-stationarity (Lindgren et al., 2011, Bolin and
639 Lindgren, 2011), for a cost similar to that of low-dimensional models. Previously, these
640 methods have successfully been used in ecology, epidemiology, and geology, but not until
641 now for datasets of the size and resolution of global historical daily temperature datasets.
642 EUSTACE development has made extensive use of these methods to create a global daily
643 mean air temperature analysis on a 0.25$^{o}$ latitude by 0.25$^{o}$ longitude grid.

644

645 We model daily mean air temperature measurements, first, as an average of each day's
646 maximum and minimum temperature and, second, as a combination of the true
647 temperature plus bias terms (including accounting for locally-correlated biases in the air
648 temperature estimates from satellite) and other errors affecting each measurement type.
649 We then assume that the true daily mean air temperature can be modelled as a linear
650 combination of three different components: a moving long-term average climatology; a
651 large-scale component representing inter-annual variability and a daily, weather-related
652 component. Each component is modelled as a linear combination of Gaussian variables and
653 is solved conditioned on the other components, starting with the climatology. The solution
654 is improved iteratively starting with the climatology, followed by the large-scale and then
655 the local component, moving from the broadest and slowest scales, to the shortest and
656 fastest. The process is then repeated. The estimation of the climatology component benefits
657 directly from the inclusion of satellite-derived data. The time-variation of the large-scale
658 component is informed largely by the long-term *in situ* measurements from ships and
659 weather stations. The correlations captured by the local component benefit from both the
660 satellite-derived and *in situ* data. Different types of errors in the input measurements are
661 associated with the individual component to which they are most relevant. For example,
662 station biases arising from non-climatic discontinuities are associated with and estimated as
663 part of the large-scale component, because breaks in the station series are identified at an
664 annual resolution. To make the computation tractable, we use a combination of local linear
665 basis functions. These basis functions combine to describe variation in space (for the daily
666 component) and, in some cases, also in time (for the large-scale component). The basis
667 functions are defined on a nested triangular mesh which also helps to speed up the

668 computation. This Bayesian method allows us to represent uncertainty in the process by
669 drawing samples from the posterior distributions of the model components. Figure 4
670 illustrates the additional information this generates and the uncertainty in different
671 components of the process for 1 January 2006.

672

673 We generate ten samples of possible representations of mean near surface air temperature
674 for each day from 1 January 1850. The usefulness of the complete field is determined
675 strongly by the availability of measurements to constrain the analysis. Therefore, where we
676 have estimated values which add no additional information (as defined by climatology or
677 large-scale uncertainties greater than a threshold), we mask these out of the analysis (white
678 areas in top right panel of Figure 4). In addition, in a few limited areas the statistical model
679 produced extreme climatological values; these were also masked. Consequently, the
680 analysis is not globally-complete.

681

682 The purpose of EUSTACE is to provide information on daily near surface air temperature to
683 enable assessments of vulnerability to its daily variations, rather than for monitoring of
684 large-scale changes on longer timescales. Nonetheless, it is important to know how the
685 global analysis compares to data sets developed for large-scale monitoring. The upper
686 panels of Figure 5 shows regional annual average near surface air temperature anomaly in
687 the EUSTACE global analysis v1.0 since 1850 for Europe and North America, together with
688 the same quantity in: a blend of CRUTEM4 (Jones et al., 2012) and HadNMAT2 (Kent et al.,
689 2013); NOAAGlobalTemp (Smith et al., 2008; Vose et al., 2012); GISTEMP (Hansen, 2010);
690 and Berkley Earth (Rohde et al., 2013a and b). From 1895 onwards, the data sets agree

691 closely. Prior to 1895, there are very few daily station measurements in the EUSTACE global
692 station data set, so the EUSTACE analysis v1.0 relies on night marine air temperature to infer
693 values over Europe. This causes a discrepancy in the EUSTACE analysis when compared to
694 the global surface temperature monitoring data sets, which are themselves instead based
695 on monthly weather station values. Monthly average data are more plentiful for the late
696 nineteenth century, having been digitised separately from daily values. Over North America,
697 the agreement is good back to 1870.

698

699 More pertinent to the aims of EUSTACE is the ability of the global analysis v1.0 to represent
700 the evolution of daily near surface air temperature at a particular location. Having withheld
701 a large number of station records from the development of the analysis, we can examine
702 how the analysis compares to these records over the course of example years. The lower
703 panels of Figure 5 show this for Cimbaj, Uzbekistan in 1975 and for Fort Nelson, Canada in
704 2003. The station records for these locations were not included in the analysis so provide an
705 independent comparator. The uncertainty in the analysis is larger for Cimbaj than for Fort
706 Nelson (shown by the envelope around the EUSTACE analysis v1.0 time series). Nonetheless,
707 in both locations, the analysis compares well on a day-to-day basis with the record of daily
708 mean near surface air temperature from GHCN-D v3.26. In particular, we see that the gaps
709 in the Fort Nelson record for 2003 are completed by the EUSTACE analysis method, which
710 uses information from other weather station records and air temperature estimated from
711 satellite to infer the missing values.

712

The EUSTACE prototype global daily air temperature ensemble is openly available via the CEDA archive (see Appendix C).

**Validation**

The EUSTACE daily air temperature estimates (both the air temperatures estimated from satellite and the global analysis) were matched with withheld validation measurements from land stations, ice stations, moored buoys, ships and ice buoys. These data were excluded from both the derivation of regression relationships between skin temperature retrievals from satellite and air temperature and from the production of the global daily analysis fields. Veal et al. (2019a) presents the full evaluation, but Figure 6 summarises the results for the EUSTACE global analysis.

Over ocean, the EUSTACE global analysis v1.0 performs well over the period 1850-2015, with a global median discrepancy (robust standard deviation, RSD) of +0.00 K (1.76 K) against withheld ship measurements (Woodruff et al., 2011) adjusted to a height of 2 m. The highest discrepancies (analysis minus validation data) are found in the Southern Ocean, although matchups are sparse here. The global analysis also performs well in most land regions with a global median discrepancy (RSD) against weather station measurements of -0.23 K (1.76 K), however seasonal median discrepancies over central Asia are high, 6-10 K in winter at some stations (these most erroneous data have been masked out of the final product). Over permanent ice domains, the global analysis performs less well, especially

735 over sea-ice: regional median discrepancies (RSDs) against ice buoy data are +1.19 K (4.60 K)
736 in the Arctic and +4.76 K (6.81 K) in the Antarctic; note that these latter two statistics are
737 affected by the sparsity of *in situ* measurements against which to compare the EUSTACE
738 analysis in these regions, but are dominated by a drift over the Poles in the analysis which
739 has largely been masked out of the final product. The regional median discrepancies (RSDs)
740 over land-ice (including the Antarctic ice-shelf) against weather station data are lower:
741 +0.37 K (4.04 K) in the Arctic and +0.47 K (2.68 K) in the Antarctic.

742

743 In addition, estimates of uncertainty are also evaluated using the withheld data. The
744 uncertainty estimates are assessed by first binning the matchup discrepancies by the value
745 of the uncertainty on the EUSTACE temperature estimate. Matchup statistics (median and
746 RSD of the matchup discrepancies) are calculated for each bin. The matchup discrepancy has
747 contributions from the uncertainty in the *in situ* reference data as well as the uncertainty on
748 the EUSTACE temperature estimate. There is also a contribution from matching two
749 different spatial scales, i.e. a point *in situ* value with the EUSTACE 0.25$^{o}$ grid box estimate.
750 The expected match up variance can be modelled as the sum of the squares of these
751 contributions. The actual and modelled matchup discrepancy variances are plotted in Figure
752 7. Assuming our estimates of the uncertainty in the reference data and the matchup process
753 are good then, if the EUSTACE uncertainty estimates are also good, for each bin the
754 matchup RSD (blue bar) should match the modelled value (dashed line). If the blue bars are
755 higher than the dashed line then the matchup discrepancy RSD exceeds the modelled value,
756 indicating that the EUSTACE uncertainty estimate is too low. The uncertainty estimates for
757 the EUSTACE global analysis v1.0 show little agreement with expectation over ocean

(overestimated and showing little variation with actual discrepancy), but good agreement over land. Since the EUSTACE analysis validates extremely well in comparison to withheld data over the ocean, this mitigates the impact of the less-effective uncertainty estimates here. Analysis uncertainties are underestimated over ice regions, particularly in the Northern Hemisphere and over Southern Hemisphere land ice; here, this arises from assumptions in the analysis method about the correlation structure of errors in the over-sampled air temperature estimates from satellite.

The EUSTACE matchup data base is available for non-commercial use (see Appendix C for details).

**Priorities for future work**

EUSTACE relies on good retrievals of surface skin temperature from infrared satellite instruments. Adequate removal of values contaminated by cloud between the surface and the sensor is crucial for accurate skin temperature retrieval, but also for correct estimation of uncertainties and for accurate estimation of air temperature from skin temperature. The skin temperature datasets currently used in EUSTACE are sporadically contaminated by uncleared clouds. Use of improved satellite retrievals will improve the EUSTACE products.

As a proof-of-concept, EUSTACE has demonstrated that inclusion of air temperatures estimated from satellite enables the more-stable estimation of the climatological

780 component of the global analysis (where biases in air temperature estimates from satellite
781 are not large or there are sufficient *in situ* measurements to inform their correction), as
782 compared to use of *in situ* measurements alone. Use of longer satellite datasets would
783 improve the amount of information available to the analysis and improve results further.
784 Since the inputs to the EUSTACE analysis were fixed, more satellite data have become
785 available (i.e. version 2 of the Arctic and Antarctic Ice Surface Temperatures from thermal
786 infrared satellite sensors (AASTI) dataset over ice, Globtemperature land surface skin
787 temperature from a further Moderate Resolution Imaging Spectroradiometer sensor, and
788 stable sea surface temperatures from the Advanced Very High Resolution Radiometer series
789 in the ESA SST CCI v2.1 dataset).

790

791 With more satellite skin temperature information would come the possibility of developing
792 and applying regionally-varying regression relationships over land. EUSTACE air temperature
793 estimates from satellite over land currently employ a global relationship determined by
794 latitude, snow cover and fractional vegetation cover; this results in some (sometimes large)
795 regionally-varying biases in the resultant air temperature estimates, which are reduced in
796 the global analysis through the additional statistical modelling undertaken there and the
797 inclusion of measurements made *in situ*.

798

799 Interactions with users have demonstrated that information on daily maximum and
800 minimum temperatures are needed in addition to the daily mean. Although EUSTACE
801 undertook modelling work to enable the production of a global analysis of maximum and
802 minimum via the mean and the diurnal temperature range, it proved impossible to pull it

803 through into production within the timeframe of the project. Methods developed
804 demonstrate promise and have applicability beyond surface temperature diurnal
805 temperature range to other non-Gaussian variables. These prototyped methods would also
806 enable full propagation of components of uncertainty with different correlation length
807 scales through to the final analysis; the current EUSTACE global analysis simplifies the
808 assumptions made to enable the calculations, but consequently results in underestimated
809 uncertainties, especially over polar regions where satellite data are plentiful.

810

811 Pull-through of the lake influence mask (see Supplemental material) as a covariate (as
812 distance from coast or altitude are currently specified) in the EUSTACE global analysis has
813 the potential to improve the air temperature fields local to large lakes (with an influence on
814 the scale of the EUSTACE grid box or larger, i.e. $0.25^{o}$ in latitude and longitude).

815

816 The availability of daily measurements made *in situ* could be increased substantially by
817 continuing the current international data rescue and digitisation efforts (see Brönnimann et
818 al. (2018), for example) and by making these and other daily measurements openly
819 available. Each new set of digitised data has the potential to improve a global analysis of air
820 temperature by better constraining the statistical modelling, particularly when targeted to
821 regions currently under-represented in the EUSTACE global station dataset (see Figure 2) or
822 in under-sampled areas of the ocean, such as the Southern Ocean (Brönnimann et al.
823 (2018)).

824

In the course of our work, we have identified the following needs to extend the current observing system: more simultaneous Voluntary Observing Ship measurements of sea-surface and near-surface air temperature (because the network is declining and provides the only means of measuring near-surface air temperature over ocean globally) and more weather station measurements of near-surface air temperature in certain surface regimes (e.g. desert, deep forest, ice, high elevation, high latitude) to both better define the relationship between skin and near-surface air temperature there and provide more data for validation.

## Summary and conclusions

The potential for future improvements outlined above notwithstanding, EUSTACE has produced a number of novel outcomes:

- a global daily station dataset with estimated locations of non-climatic discontinuities and their likelihood;
- a pan-European station dataset homogenised to reduce the impact of non-climatic discontinuities and gridded ensemble analyses for Europe;
- consistently-estimated components of uncertainty in satellite skin temperature retrievals over different surfaces of Earth;
- air temperature estimates from satellite for each surface (land, ocean and ice) with propagated uncertainty components;

- a deeper understanding of the role of lakes in responding to and influencing surrounding surface air temperature;
- a global, multi-decadal daily analysis of surface air temperature incorporating both measurements made *in situ* and estimated from satellite data; and
- validation of products using withheld reference data.

These data have been made publicly available, where not restricted by source data licenses, both for direct use and to form the basis of future onward developments (see Appendix C for details).

## APPENDIX A

## The EUSTACE team

The EUSTACE consortium included 9 organisations:

1) Met Office (United Kingdom)
2) The University of Reading (United Kingdom)
3) Science and Technology Facilities Council (United Kingdom)
4) University of Leicester (United Kingdom)
5) Koninklijk Nederlands Meteorologisch Instituut-KNMI (Netherlands)
6) University of Bern (Switzerland)
7) University of Bath (United Kingdom)
8) Danmarks Meteorologiske Institut (Denmark)
9) University of Edinburgh (United Kingdom)

An External Expert Advisory Board comprised: Prof. Peter Thorne (University of Ireland, Maynooth); Dr. Elizabeth Kent (National Oceanography Centre, Southampton); and Prof. Doug Nychka (National Centers for Atmospheric Research and Colorado School of Mines).

## APPENDIX B

## EUSTACE input data

The EUSTACE data products are based on a number of input data sources, summarised in Tables A1-A3.

Table A1 here

Table A2 here

Table A3 here

## APPENDIX C

## EUSTACE products

The EUSTACE data products have been catalogued in the Centre for Environmental Data Analysis (CEDA) archive, with individual download pages pointing to the data. Two products, the European homogenised data and the gridded European dataset, which also form part of the European Climate Assessment & Dataset (ECA&D) are made available separately via ECA&D.

The EUSTACE data products and their availability and licenses are summarised in the table below.

Table A4 here

Data are made available on an open license (Open Government Licence http://www.nationalarchives.gov.uk/doc/open-government-licence/version/3/) where possible. For the station datasets and the matchup data base, this was not possible due to the licensing conditions of the input datasets, which meant they could only be made available for non-commercial use. These have been made available under a non-commercial license (Non-Commercial Government http://www.nationalarchives.gov.uk/doc/non-commercial-government-licence/version/2/).

In addition, EUSTACE has produced:

- User requirements reports;
- Product user guides, including detailed guidance on uncertainties and information content in the products; and
- Peer-reviewed journal articles.

Links to all of these can be found on the EUSTACE website (https://www.eustaceproject.org).

916 Acknowledgments

917 The EUSTACE project received funding from the European Union's Horizon 2020 research
918 and innovation programme under grant agreement 640171. We thank Professor Doug
919 Nychka for his advice throughout EUSTACE as part of the External Expert Advisory Board and
920 Gary Corlett for validation of interim versions of the EUSTACE air temperature estimates
921 over ocean. We also thank Esther Conway for her work on the data management plan and
922 Roy Mandemakers for provision of a step-by step-guide for using the Climate4Impact portal
923 as part of the EUSTACE user guides. ECK contribution was funded under NERC grant
924 NE/J020788/1. We thank three anonymous reviewers for their comments which improved
925 the manuscript.

926

927

928 References

929

930 Aguilar, E., M. Brunet, J. Sigró, F. S. Rodrigo, Y. L. Rico, and D. R. Alvarez, 2008:
931 Homogenization of Spanish temperature series on a daily resolution: A step forward
932 towards an analysis of extremes in the Iberian Peninsula. Proc. Seventh European Conf. on
933 Applied Climatology, Amsterdam, the Netherlands, European Meteor. Soc., A-00-697.

934

935 Auchmann, R and S. Brönnimann, 2012: A physics-based correction model for homogenizing
936 sub-daily temperature series. J. Geophys. Res. 117, D17119,
937 https://doi.org/10.1029/2012JD018067

938

939 Banerjee, S., Gelfand, A. E., Finley, A. O., Sang, H., 2008: Gaussian Predictive Process Models
940 for Large Spatial Datasets. J. Roy. Statist. Soc. B, 70(4), 825–848.

941

942 Bessembinder, J., 2016: User requirement specification for product design, EUSTACE
943 Deliverable 4.1,
944 https://www.eustaceproject.org/eustace/static/media/uploads/Deliverables/eustace_d4-
945 1.pdf

946

947 Bessembinder, J., N. Rayner, D. Ghent, K. Madsen and J. Mitchelson, 2017: Report on user
948 requirements: results from second round of user consultations, EUSTACE Deliverable 4.9,

https://www.eustaceproject.org/eustace/static/media/uploads/Deliverables/eustace_d4-9.pdf

Bolin D., Lindgren F., 2011: Spatial Models Generated by Nested Stochastic Partial Differential Equations, with an Application to Global Ozone Mapping, The Annals of Applied Statistics, 5(1), 523–550.

Brandsma, T. and G.P. Konnen, 2006: Application of nearest-neighbor resampling for homogenizing temperature records on a daily to sub-daily level, Int. J. Climatol., 26, 75-89, https://doi.org/10.1002/joc.1236.

Brönnimann, S., and Coauthors, 2018: Observations for Reanalyses, Bull. Amer. Meteorol. Soc., 99, 1851–1866, https://doi.org/10.1175/BAMS-D-17-0229.1

Brugnara Y., R. Auchmann, S. Brönnimann, A. Bozzo, D. Cat Berro and L. Mercalli, 2016: Trends of mean and extreme temperature indices since 1874 at low-elevation sites in the Southern Alps. J. Geophys. Res., 121, 3304–3325, https://doi.org/10.1002/2015JD024582

Brugnara, Y., E. Good, A. A. Squintu, G. van der Schrier, S. Brönnimann, 2019: The EUSTACE global land station daily air temperature dataset. Geoscience Data Journal, https://doi.org/10.1002/gdj3.81

970

971 Brunet, M., and Coauthors, 2006: The development of a new dataset of Spanish daily
972 adjusted temperature series (SDATS) (1850– 2003), Int. J. Climatol., 26, 1777-1802,
973 https://doi.org/ 10.1002/joc.1338

974

975 Buizza, R. and Coauthors, 2018: The EU-FP7 ERA-CLIM2 project contribution to advancing
976 science and production of Earth System climate reanalyses, Bull. Amer. Meteor. Soc., 99,
977 1003-1014, https://doi.org/10.1175/BAMS-D-17-0199.1

978

979 Bulgin, C. E., C. J., Merchant, D., Ghent, L., Klueser, T., Popp, C. Poulsen, and L. Sogacheva,
980 2018: Quantifying uncertainty in satellite-retrieved land surface temperature from cloud
981 detection errors, Remote Sensing, 10 (4). 616. ISSN 2072-4292,
982 https://doi.org/10.3390/rs10040616

983

984 Caesar, J., L. Alexander, and R. Vose, 2006: Large-scale changes in observed daily maximum
985 and minimum temperatures: Creation and analysis of a new gridded data set, J. Geophys.
986 Res., 111, D05101, https://doi.org/10.1029/2005JD006280

987

988 Carrea, L., and Coauthors, 2019: Lake surface temperature [in “State of the Climate 2018”].
989 Bull. Amer. Meteor. Soc., 100 (9), S13-S14, doi:10.1175/2019BAMSStateoftheClimate.1

990

Caussinus, H. and O. Mestre, 2004: Detection and correction of artificial shifts in climate series, J. R. Stat. Soc., 53(3), 405-425.

Cornes, R. C., G. van der Schrier, E. J. M. Besselaar, and P. D. Jones, 2018: An ensemble version of the E-OBS temperature and precipitation data sets. J. Geophys. Res. (Atmospheres), 123, 9391– 9409, https://doi.org/10.1029/2017JD028200

Cristóbal, J., M. Ninyerola, and X. Pons, 2008: Modeling air temperature through a combination of remote sensing and GIS data, J. Geophys. Res., 113, D13106, https://doi.org/10.1029/2007JD009318.

Dunn, R. J. H., K. M. Willett, D. E. Parker, and L. Mitchell, 2016: Expanding HadISD: quality-controlled, sub-daily station data from 1931, Geosci. Instrum. Method. Data Syst., 5, 473-491, https://doi.org/10.5194/gi-5-473-2016

EUMETSAT, 2014: CORE-CLIMAX System Maturity Matrix Instruction Manual, 34pp.

Furrer, R., Genton, M.G., Nychka, D., 2006: Covariance tapering for interpolation of large spatial datasets. J. Comput. Graph. Statist, 15, 502–523.

1011 Ghent D., K. Veal, T. Trent, E. Dodd, H. Sembhi and J. Remedios, 2019: A new approach to
1012 defining uncertainties for MODIS land surface temperature, Remote Sens., 11,
1013 https://doi.org/10.3390/rs11091021

1014

1015 Good, E. J., 2016: An in situ-based analysis of the relationship between land surface "skin"
1016 and screen-level air temperatures, J. Geophys. Res. Atmos., 121, 8801–8819,
1017 https://doi.org/10.1002/2016JD025318.

1018

1019 Hansen, J., R. Ruedy, M. Sato, and K. Lo, 2010: Global surface temperature change, Rev.
1020 Geophys., 48, RG4004, https://doi.org/10.1029/2010RG000345.

1021

1022 Harris, I., Jones, P.D., Osborn, T.J. and Lister, D.H., 2013: Updated high-resolution grids of
1023 monthly climatic observations - the CRU TS3.10 dataset, Int. J. Climatol., 34, 623-642,
1024 https://doi.org/10.1002/joc.3711.

1025

1026 Hartmann, D.L., A.M.G. Klein Tank, M. Rusticucci, L.V. Alexander, S. Brönnimann, Y. Charabi,
1027 F.J. Dentener, E.J. Dlugokencky, D.R. Easterling, A. Kaplan, B.J. Soden, P.W. Thorne, M. Wild
1028 and P.M. Zhai, 2013: Observations: Atmosphere and Surface. In: Climate Change 2013: The
1029 Physical Science Basis. Contribution of Working Group I to the Fifth Assessment Report of
1030 the Intergovernmental Panel on Climate Change [Stocker, T.F., D. Qin, G.-K. Plattner, M.
1031 Tignor, S.K. Allen, J. Boschung, A. Nauels, Y. Xia, V. Bex and P.M. Midgley (eds.)]. Cambridge
1032 University Press, Cambridge, United Kingdom and New York, NY, USA.

1033

1034 Høyer, J. L., E. Good, P. Nielsen-Englyst, K. S. Madsen, I. Woolway, J. Kennedy, 2018: Report
1035 on the relationship between satellite surface skin temperature and surface air temperature
1036 observations for oceans, land, sea ice and lakes, EUSTACE Deliverable 1.5,
1037 https://www.eustaceproject.org/eustace/static/media/uploads/d1.5_revised.pdf

1038

1039 Hunziker, S., and Coauthors, 2017: Identifying, attributing, and overcoming common data
1040 quality issues of manned station observations. Int. J. Climatol., 37, 4131-4143.

1041

1042 Jones, P. D., D. H. Lister, T. J. Osborn, C. Harpham, M. Salmon, and C. P. Morice, 2012:
1043 Hemispheric and large-scale land surface air temperature variations: An extensive revision
1044 and an update to 2010. J. Geophys. Res., 117, doi:10.1029/2011JD017139

1045

1046 Kennedy, J. J. and E. C. Kent, 2019: Estimating the climatological mean and spatial
1047 covariance of air-sea temperature differences, in prep for Geophys. Res. Lett.

1048

1049 Kent, E.C., Rayner, N.A., Berry, D.I., Saunby, M., Moat, B.I., Kennedy, J.J., Parker, D.E., 2013:
1050 Global analysis of night marine air temperature and its uncertainty since 1880: The
1051 HadNMAT2 data set. J. Geophys. Res., 118, 1281–1298, https://doi.org/10.1002/jgrd.50152

1052

Kilibarda, M., T. Hengl, G. B. M. Heuvelink, B. Gräler, E. Pebesma, M. Perčec Tadić, and B. Bajat, 2014: Spatio-temporal interpolation of daily temperatures for global land areas at 1 km resolution. J. Geophys. Res., 119, 2294–2313, https://doi.org/10.1002/2013JD020803.

Klein-Tank, A. M. G., and Coauthors, 2002: Daily dataset of 20th-century surface air temperature and precipitation series for the European Climate Assessment. International Journal of Climatology, 22, 1441-1453.

Kuglitsch, F.G., A. Toreti, E. Xoplaki, P. M. Della-Marta, J. Luterbacher, and H. Wanner, 2009: Homogenization of daily maximum temperature series in the Mediterranean. J. Geophys. Res., 114, https://doi.org/10.1029/2008JD011606.

Kushnir, Y., A.A. Scaife and Coauthors, 2019: Towards operational predictions of the near-term climate, Nature Climate Change, 9, 94-101, http://doi.org/10.1038/s41558-018-0359-7

Jones, G.S. and J.J. Kennedy, 2017: Sensitivity of Attribution of Anthropogenic Near-Surface Warming to Observational Uncertainty, J. Climate, 30, 4677-4691, http://doi.org/10.1175/JCLI-D-16-0628.1

1072 Lindgren, F., H. Rue, and J. Lindström, 2011: An explicit link between Gaussian fields and
1073 Gaussian Markov random fields: the stochastic partial differential equation approach, J. Roy.
1074 Statist. Soc. B, 73(4), 423–498, https://doi.org/10.1111/j.1467-9868.2011.00777.x

1075

1076 Menne, M.J., I. Durre, R. S. Vose, B. E. Gleason, and T. G. Houston, 2012: An Overview of the
1077 Global Historical Climatology Network-Daily Database. J. Tech., 29, 897-910,
1078 http://doi.org/10.1175/JTECH-D-11-00103.1

1079

1080 Merchant C. J., and Coauthors, 2013: The surface temperatures of Earth: steps towards
1081 integrated understanding of variability and change, Geosci. Instrum. Method. Data Syst., 2,
1082 305–321, https://doi:10.5194/gi-2-305-2013

1083

1084 Merchant, C. J., and Coauthors, 2014: Sea surface temperature datasets for climate
1085 applications from Phase 1 of the European Space Agency Climate Change Initiative (SST CCI),
1086 Geosci. Data Journal, https://doi.org/10.1002/gdj3.20

1087

1088 Merchant, C., D. Ghent, J. Kennedy, E. Good, and J. Høyer, 2015: Common approach to
1089 providing uncertainty estimates across all surfaces, EUSTACE Deliverable 1.2, 20 pp,
1090 https://www.eustaceproject.org/eustace/static/media/uploads/Deliverables/eustace_d1-
1091 2.pdf

1092

1093 Morice, C. P., J. J. Kennedy, N. A. Rayner, and P. D. Jones, 2012: Quantifying uncertainties in
1094 global and regional temperature change using an ensemble of observational estimates: The
1095 HadCRUT4 dataset, J. Geophys. Res., 117, http://doi.org/10.1029/2011JD017187.

1096

1097 Nielsen-Englyst, P., Høyer J. L., Madsen, K. S., Tonboe, R., and Dybkjær, G., 2019a: Deriving
1098 Arctic 2-m air temperatures from satellite, submitted to The Cryosphere,
1099 https://doi.org/10.5194/tc-2019-126

1100

1101 Nielsen-Englyst, P., Høyer, J. L., Madsen, K. S., Tonboe, R., Dybkjær, G., and Alerskans, E.,
1102 2019b: In situ observed relationships between skin temperatures and 2 m air temperatures
1103 in the Arctic, The Cryosphere, http://doi.org/10.5194/tc-13-1005-2019

1104

1105 Osborn, T.J., P.D. Jones and M. Joshi, 2017: Recent United Kingdom and global temperature
1106 variations, Weather, 72, 323-329, http://doi.org/10.1002/wea.3174

1107

1108 Peterson, T.C., and Coauthors, 1998: Homogeneity adjustments of in situ atmospheric
1109 climate data: A review. Int. J. Climatol., 18, 1493-1517, http://doi.org/10.1002/(SICI)1097-
1110 0088(19981115)18:13<1493::AID-JOC329>3.0.CO;2-T

1111

Rayner, N.A., 2019: Final verified products delivered to CEMS for verification. EUSTACE Deliverable 2.6, https://www.eustaceproject.org/eustace/static/media/uploads/d_2.6_final.pdf

Rennie, J. J., and Coauthors (2014). The international surface temperature initiative global land surface databank: Monthly temperature data release description and methods. Geoscience Data Journal, 1, 75-102.

Rohde R., R. A. Muller, R. Jacobsen, E. Muller, S. Perlmutter, A. Rosenfeld, J. Wurtele, D. Groom, and C. Wickham, 2013a: A New Estimate of the Average Earth Surface Land Temperature Spanning 1753 to 2011. Geoinfor Geostat: An Overview 1:1, http://doi.org/10.4172/2327-4581.1000101

Rohde R., R. Muller, R. Jacobsen, S. Perlmutter, A. Rosenfeld, J. Wurtele, J. Curry, C. Wickham, and S. Mosher, 2013b: Berkeley Earth Temperature Averaging Process. Geoinfor Geostat: An Overview 1:2, http://doi.org/10.4172/2327-4581.1000103

Rue H., S. Martino, F. Lindgren, D. Simpson, A. Riebler, 2013: R-INLA: Approximate Bayesian Inference using Integrated Nested Laplace Approximations. Trondheim, Norway. URL http://www.r-inla.org/.

1133 Sánchez-Lugo, A., P. Berrisford, C. Morice and J.P. Nicolas, 2019: Global surface temperature
1134 [in "State of the Climate 2018"]. Bull. Amer. Meteor. Soc., 100 (9), S11-S12,
1135 doi:10.1175/2019BAMSStateoftheClimate.1

1136

1137 Smith, T.M., R.W. Reynolds, T.C. Peterson, and J. Lawrimore, 2008: Improvements to NOAA's
1138 historical merged land–ocean surface temperatures analysis (1880–2006). J. Climate, 21,
1139 2283–2296, http://doi.org/10.1175/2007JCLI2100.1.

1140

1141 Sohrabinia, M. , P. Zawar-Reza and W. Rack, 2014: Spatio-temporal analysis of the
1142 relationship between LST from MODIS and air temperature in New Zealand, Theor. Appl.
1143 Climatol., DOI 10.1007/s00704-014-1106-2.

1144

1145 Squintu, A.A., G. van der Schrier, Yuri Brugnara, Albert Klein Tank, 2019a: Homogenization of
1146 daily temperature series in the European Climate Assessment & Dataset, Int. J. Climatol.,
1147 39:1243-1261. http://doi.org/10.1002/joc.5874

1148

1149 Squintu, A. A., G. van der Schrier, E. J. M. van den Besselaar, R. C. Cornes, A. Klein Tank,
1150 2019b: Building long homogeneous temperature series across Europe: a new approach for
1151 the blending of neighboring series, submitted to J. Appl. Meteorol. Clim.

1152

1153 Stickler, A., and Coauthors, 2014: ERA-CLIM: historical surface and upper-air data for future
1154 reanalyses. Bull. Amer. Meteorol. Soc., 95, 1419-1430.

1155

1156 Toreti, A., F. G. Kuglitsch, E. Xoplaki, and J. Luterbacher, 2012: A novel approach for the
1157 detection of inhomogeneities affecting climate time series. J. Appl. Meteorol. Clim., 51, 317-
1158 326, http://doi.org/10.1175/JAMC-D-10-05033.1.

1159

1160 Trewin, B., 2013: A daily homogenized temperature data set for Australia. Int. J. Climatology,
1161 33, 1510-1529.

1162

1163 Veal, K., 2019a: Validation report for the final in-filled EUSTACE surface air temperature
1164 product, EUSTACE Deliverable 3.5

1165

1166 Veal, K., 2019b: Intercomparison report for the final in-filled EUSTACE surface air
1167 temperature product, EUSTACE Deliverable 3.4

1168

1169 Venema, V., et al, 2012: Detecting and repairing inhomogeneities in datasets, assessing
1170 current capabilities. Bull. Am. Meteorol. Soc., 93, no. 7, pp. 951-954.

1171

1172 Vincent, L., X. Zhang, B. R. Bonsall, W. D. Hogg, 2002: Homogenization of Daily Temperatures
1173 over Canada. J. Climate, 15, 1322-1334.

1174

1175 Vose, R.S., and Coauthors, 2012: NOAA's merged land-ocean surface temperature analysis.
1176 Bull. Amer. Meteor. Soc., 93, 1677–1685, http://doi.org/10.1175/BAMS-D-11-00241.1.

1177

1178 Walters, D. and Coauthors, 2019: The Met Office Unified Model Global Atmosphere 7.0/7.1
1179 and JULES Global Land 7.0 configurations. Geoscientific Model Development, 12, 1909-1963,
1180 http://doi.org/10.5194/gmd-12-1909-2019

1181

1182 Xu, X. and Coauthors 2019: The effects of temperature on human mortality in a Chinese city:
1183 burden of disease calculation, attributable risk exploration, and vulnerability identification.
1184 Int. J. Biometeor., 63, 1319-1329, http://doi.org/10.1007/s00484-019-01746-6

1185

1186

1187 Wang, X. L., 2008: Accounting for autocorrelation in detecting mean shifts in climate data
1188 series using the penalized maximal t or f test. J. Appl. Meteorol. Clim., 47, 2423-2444,
1189 http://doi.org/10.1175/2008JAMC1741.1.

1190

1191 Weedon, G.P., and Coauthors, 2011: Creation of the WATCH Forcing Data and Its Use to
1192 Assess Global and Regional Reference Crop Evaporation over Land during the Twentieth
1193 Century, J Hydromet, 12, 823-848, http://doi.org/10.1175/2011JHM1369.1

1194

1195 Wikle, C. K., 2010: In Handbook of Spatial Statistics, chapter Low-rank Representations for
1196 Spatial Processes, pp. 107–118. Chapman and Hall/CRC, Boca Raton, FL.

1197

1198 Woodruff, S. D., and Coauthors, 2011: ICOADS Release 2.5: extensions and enhancements to
1199 the surface marine meteorological archive. Int. J. Climatol., 31, 951-967,
1200 http://doi.org/10.1002/joc.2103

1201

1202 Woolway, R. I., and Coauthors, 2016: Lake surface temperatures. [in "State of the Climate in
1203 2015"]. Bull. Amer. Meteor. Soc., 97 (8), S17-S18,
1204 https://doi.org/10.1175/2016BAMSStateoftheClimate.1

1205

1206 Woolway, R.I. and C. Merchant, 2017: Amplified surface temperature response of cold, deep
1207 lakes to inter-annual air temperature variability. Nature Scientific Reports, 7,
1208 http://doi.org/10.1038/s41598-017-04058-0.

1209

1210 Woolway, R. I., et al., 2017a: Lake surface temperature [in "State of the Climate in 2016"].
1211 Bull. Amer. Meteor. Soc., 98 (8), S13–S14,
1212 http://doi.org/10.1175/2017BAMSStateoftheClimate.1.

1213

1214 Woolway, R. I., and Coauthors, 2017b: Latitude and lake size are important predictors of over-
1215 lake atmospheric stability, Geophys. Res. Lett., 44, http://doi.org/10.1002/2017GL073941

1216

1217 Woolway, R.I., Dokulil, M. T., Marszelewski, W., Schmid, M., Bouffard, D., Merchant, C. J.,
1218 2017c: Warming of Central European lakes and their response to the 1980s climate regime
1219 shift. Climatic Change, 142, 505-520, http://doi.org/10.1007/s10584-017-1966-4.

1220

1221 Woolway, R. I., P. Meinson, P. Nõges, I. D. Jones and A. Laas, 2017d: Atmospheric stilling leads
1222 to prolonged thermal stratification in a large shallow polymictic lake, Climatic Change, 141,
1223 759–773, http://doi.org/10.1007/s10584-017-1909-0

1224

1225 Woolway, R. I. and Merchant, C. J., 2018: Intra-lake heterogeneity of thermal responses to
1226 climate change: A study of large Northern Hemisphere lakes. J. Geophys. Res., 123,
1227 http://doi.org/10.1002/2017JD027661

1228

1229 Woolway, R. I., and Coauthors, 2018a: Lake surface temperature [in "State of the Climate in
1230 2017"]. Bull. Amer. Meteor. Soc., 99(8), S13–S15,
1231 http://doi.org/10.1175/2018BAMSStateoftheClimate.

1232

1233 Woolway, R. I., and Coauthors, 2018b: Geographic and temporal variation in turbulent heat
1234 loss from lakes: A global analysis across 45 lakes. Limnol. Oceanogr., 63, 2436-2449,
1235 http://doi.org/10.1002/lno.10950

1236

Xu, W., Q. Li, X. L. Wang, S. Yang, L. Cao, and Y. Feng, 2013: Homogenization of Chinese daily surface air temperatures and analysis of trends in the extreme temperature indices, J. Geophys. Res., 118, http://doi.org/10.1002/jgrd.50791.

1240 Tables.

1241

1242 Table A1. Satellite data on which EUSTACE products are based and period of data used.

1243

| Satellite instrument | Satellite programme | Variables used | Data producers |
|---|---|---|---|
| Along Track Scanning Radiometer (ATSR) series, 1991-2012 | ESA | Sea surface temperature at 0.2m depth on 0.25° latitude by 0.25° longitude grid | ESA CCI SST, experimental v1.2 (A)ATSR Level 3C data product. See Appendix C for data access. |
| Advanced Very High Resolution Radiometer (AVHRR) series, 2000-2009 | NOAA | Ice surface skin temperature on instrument swath | AASTI v1.0 dataset generated by Met Norway and DMI within the NORMAPP and the NACLIM projects. See Appendix C for data access. |

| | | | |
|---|---|---|---|
| Moderate Resolution Imaging Spectroradiometer (MODIS) Aqua + Terra, 2000-2016 | NASA | Land surface skin temperature on instrument swath | USGS/NASA (via ESA GlobTemperature). MODIS Collection 6 radiances downloaded from the NASA Level-1 and Atmosphere Archive & Distribution System Distributed Active Archive Center [https://ladsweb.modaps.eosdis.nasa.gov/]. See Appendix C for data access. |

1244

1245

1246 Table A2. Weather station air temperature measurements on which EUSTACE products are

1247 based and period of data used.

1248

| Dataset | Link | Reference |
|---|---|---|
| Global Historical Climatology Network – Daily (GHCN-D), version 3.22, 1850-2015 | http://doi.org/10.7289/V5D21VHZ | Menne et al., 2012 |
| International Surface Temperature Initiative (ISTI), v1.00 stage 2, 1850-2015 | http://www.surfacetemperatures.org/databank | Rennie et al., 2014 |
| European Climate Assessment & Dataset (ECA&D), 1950-2015 | https://www.ecad.eu/ | Klein-Tank et al., 2002 |
| Data rescued by ERA-CLIM project, various | | Stickler et al., 2014 |
| DECADE project, 1931 onwards | http://www.geography.unibe.ch/research/climatology_group/research_projects/decade/index_eng.html | Hunziker et al., 2017 |
| Southern Alps homogenized, 1871-2015 | | Brugnara et al 2016 |
| Data from the national weather service of Argentina | Servicio Meteorologico Nacional Argentina | |

1249

1250 Table A3. Marine *in situ* measurements on which EUSTACE products are based and period of

1251 data used.

1252

| Dataset | Link | Reference |
|---|---|---|
| HadNMAT2 observations, derived from ICOADS release 2.5.1, 1850-2010 | http://www.metoffice.gov.uk/hadobs/hadnmat2/ | Kent et al., 2013 |

1253

1254 Table A4. EUSTACE products and their access and licensing information

1255

| Short name | Descriptive name | Dataset link | License |
|---|---|---|---|
| Satellite skin temperatures | | | |
| Global satellite land surface temperature, v2.1 | EUSTACE / GlobTemperature: Global clear-sky land surface temperature from MODIS Aqua on the satellite swath with estimates of uncertainty | http://catalogue.ceda.ac.uk/uuid/0f1a958a130547febd40057f5ec1c837 | Open |

| | | | |
|---|---|---|---|
| | components, v2.1, 2002-2016 | | |
| | EUSTACE / GlobTemperature: Global clear-sky land surface temperature from MODIS Terra on the satellite swath with estimates of uncertainty components, v2.1, 2000-2016 | http://catalogue.ceda.ac.uk/uuid/655866af94cd4fa6af67809657b275c3 | Open |
| Global satellite ice surface temperature, v1.1 | EUSTACE / AASTI: Global clear-sky ice surface temperature from the AVHRR series on the satellite swath with estimates of uncertainty components, v1.1, 2000-2009 | https://catalogue.ceda.ac.uk/uuid/60b820fa10804fca9c3f1ddfa5ef42a1 | Open |
| Global satellite sea surface | EUSTACE / CCI: Global clear-sky sea surface temperature from the (A)ATSR series at 0.25 | https://catalogue.ceda.ac.uk/uuid/b8285969426a4e00b74814342 | Open |

| | | | |
|---|---|---|---|
| temperature, v1.2 | degrees with estimates of uncertainty components, v1.2, 1991-2012 | | |
| Surface air temperatures from *in situ* measurements | | | |
| European station measure-ments | EUSTACE/ECA&D: European land station daily air temperature measurements, homogenised | https://catalogue.ceda.ac.uk/uuid/81784e3642bd465aa69c7fd40ffe1b1b | Non-commercial use only |
| Global Station Measure-ments | EUSTACE: Global land station daily air temperature measurements with non-climatic discontinuities identified, for 1850-2015 | http://catalogue.ceda.ac.uk/uuid/7925ded722d743fa8259a93acc7073f2 | Non commercial use only |
| Validation match up database, v1.0 | EUSTACE: coincident daily air temperature estimates and reference measurements, for validation, 1850-2015, v1.0 | https://catalogue.ceda.ac.uk/uuid/4b34a2c6890f4e518cacc88911193354 | Non-commercial use only |

| | | | |
|---|---|---|---|
| E-OBS | EUSTACE / E-OBS: Gridded European surface air temperature based on homogenised land station records since 1950 | https://catalogue.ceda.ac.uk/uuid/b2670fb9d6e14733b303865c85c65d | Non commercial use only |
| | Surface air temperature estimates from statistical analysis | | |
| Air temperature estimates from satellite, v1.0 | EUSTACE: Globally gridded clear-sky daily air temperature estimates from satellites with uncertainty estimates for land, ocean and ice, 1995-2016 | https://catalogue.ceda.ac.uk/uuid/f883e197594f4fbaae6edebafb3fddb3 | Open |
| Global air temperature estimates, v1.0 | EUSTACE: Global daily air temperature combining surface and satellite data, with uncertainty estimates, for 1850-2015, v1.0 | https://catalogue.ceda.ac.uk/uuid/468abcf18372425791a31d15a41348d9 | Open |

1256

1257

1258 Figures

1259

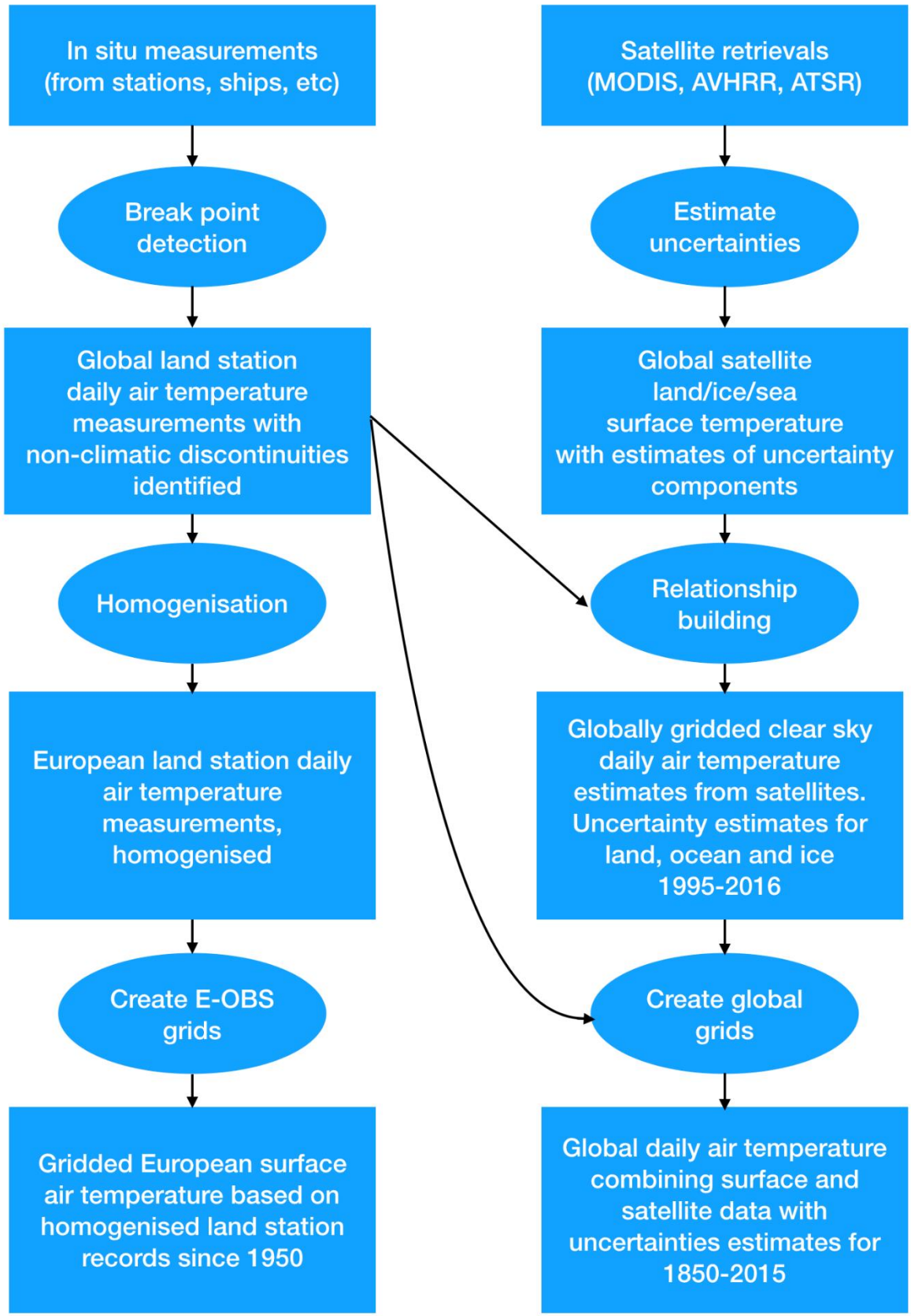
In situ measurements (from stations, ships, etc)
Break point detection
Global land station daily air temperature measurements with non-climatic discontinuities identified
Homogenisation
European land station daily air temperature measurements, homogenised
Create E-OBS grids
Gridded European surface air temperature based on homogenised land station records since 1950
Satellite retrievals (MODIS, AVHRR, ATSR)
Estimate uncertainties
Global satellite land/ice/sea surface temperature with estimates of uncertainty components
Relationship building
Globally gridded clear sky daily air temperature estimates from satellites. Uncertainty estimates for land, ocean and ice 1995-2016
Create global grids
Global daily air temperature combining surface and satellite data with uncertainties estimates for 1850-2015

1260

Figure 1. Schematic of work undertaken in the EUSTACE project. Top-most boxes denote input data. Ovals denote new development. Other boxes denote EUSTACE products (see also Appendix C). Connections between different components are indicated by arrows.

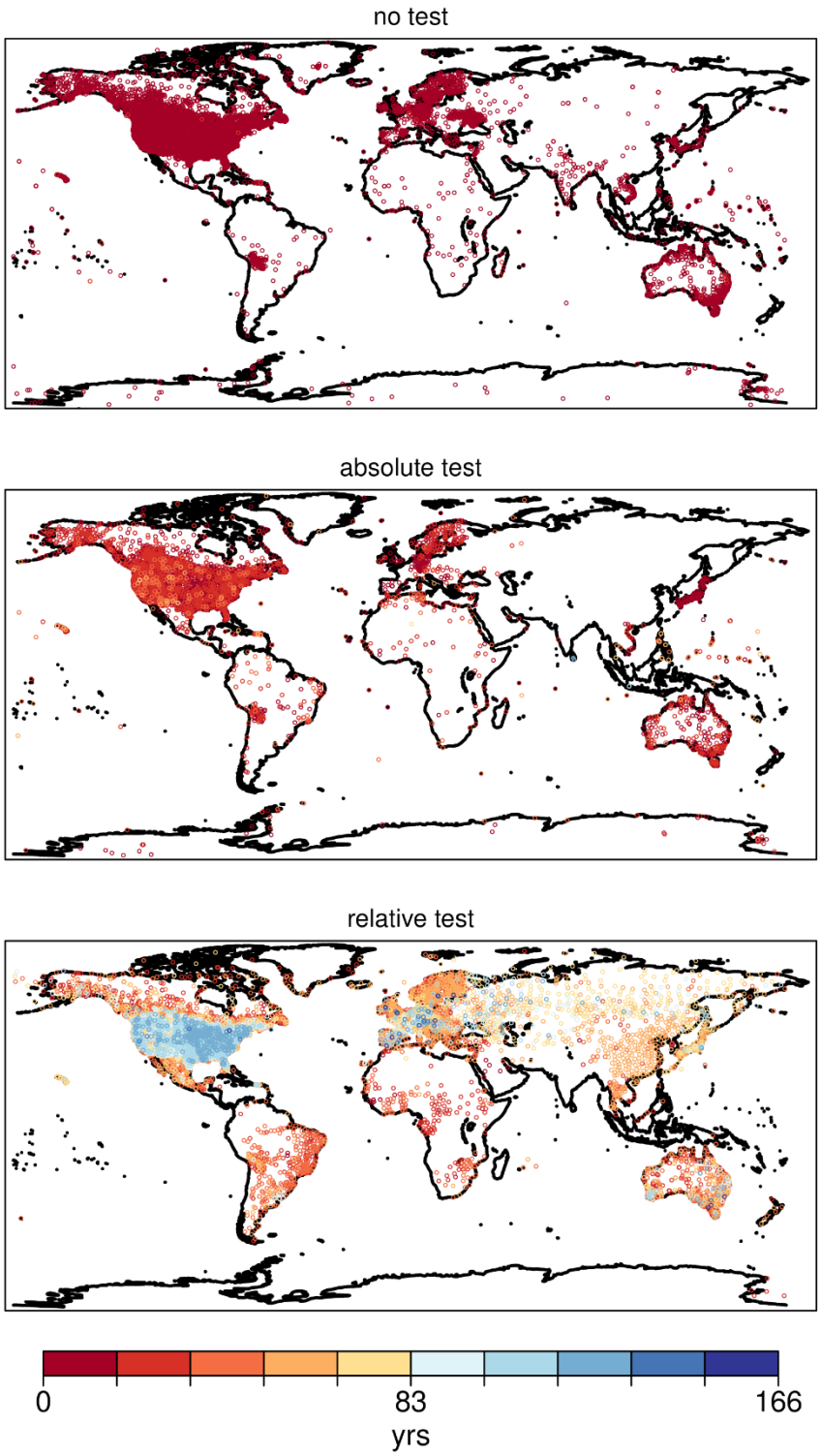


Figure 2. Map of weather stations included in the EUSTACE global station air temperature data set and break-detection tests applied (see text). Color of symbols represents length of daily surface air temperature record available. Top: no test applied. These stations are those

which have records shorter than 10 years. Middle: only absolute test applied. Bottom: relative test applied.

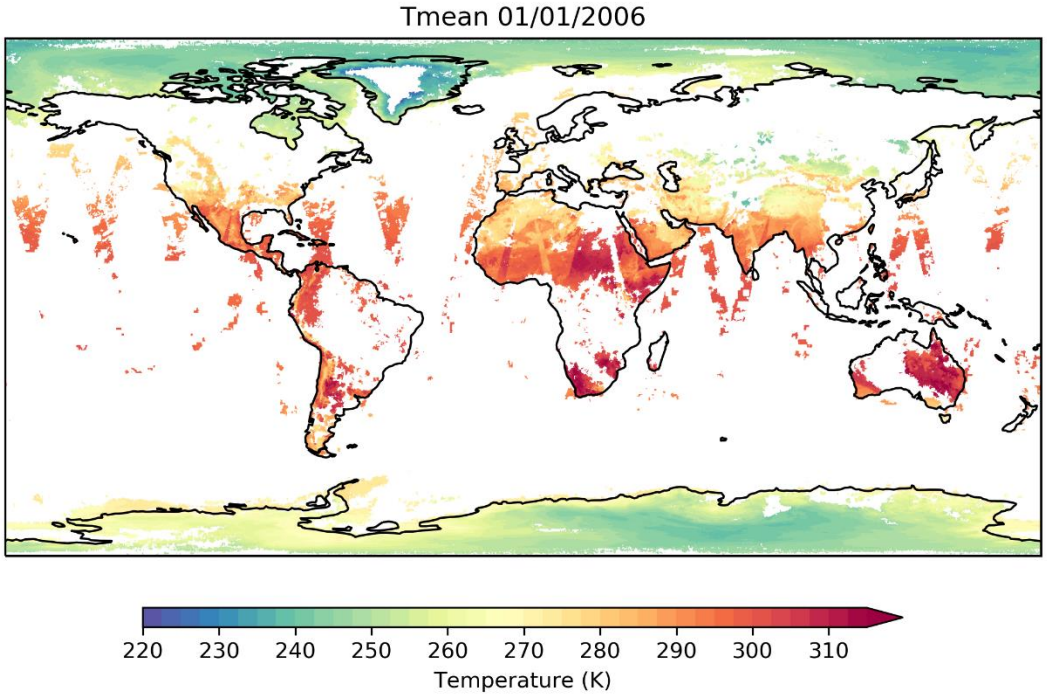


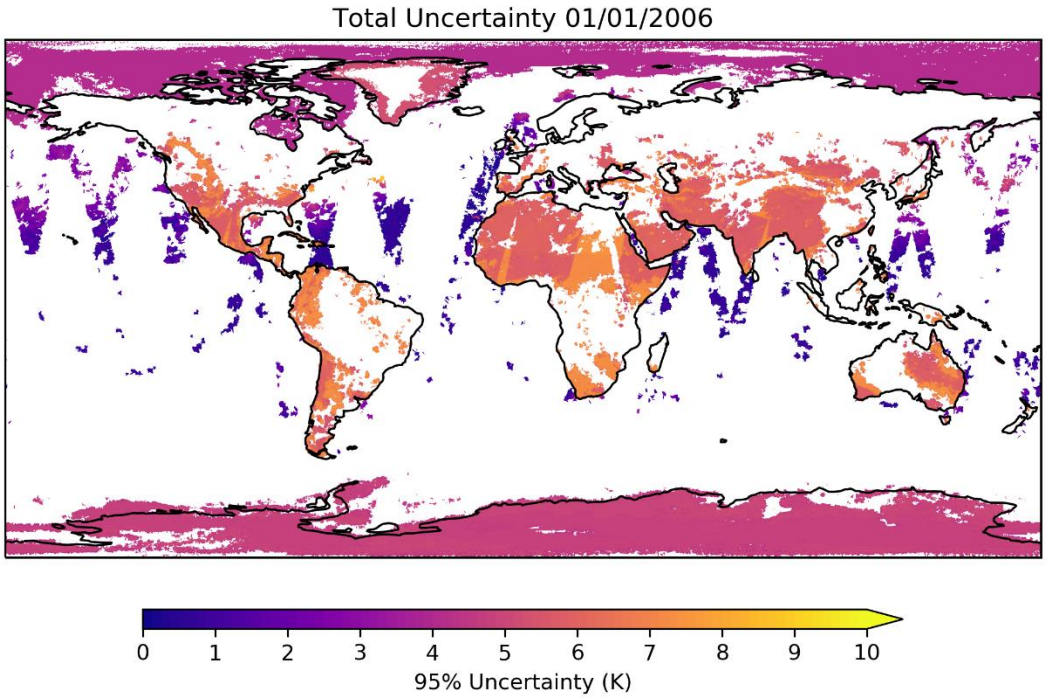


Figure 3. EUSTACE air temperature estimates from satellite. (Top) daily mean air temperatures (K) estimated for 01 01 2006. (Bottom) combined uncertainty (K).

1275

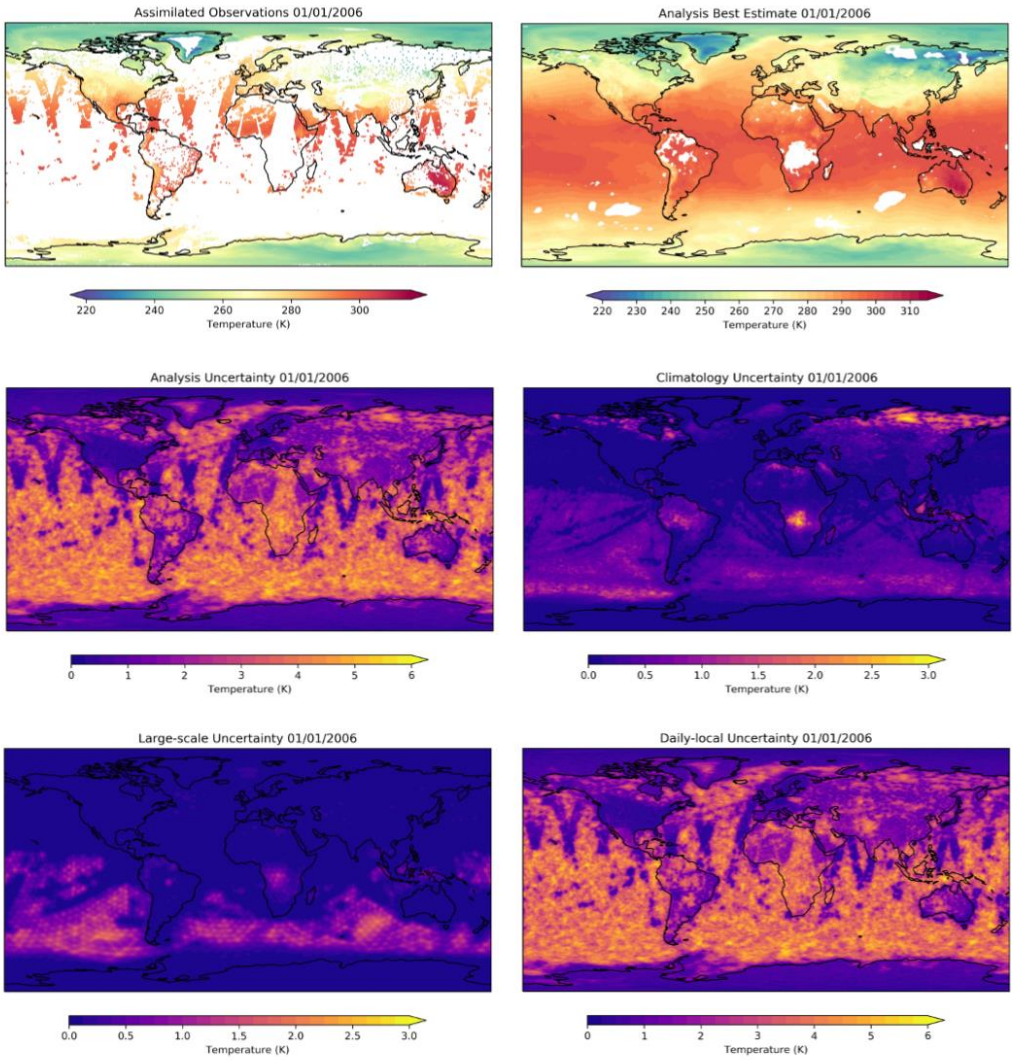


1276

1277 Figure 4. Air temperature (K) for 01 01 2006. Top left: input observations of air temperature
1278 (K). Top right: best guess combined *in situ* and satellite measurements from EUSTACE
1279 statistical infilling (K). Areas with climatology or large-scale component uncertainty above a
1280 threshold are masked. Middle left: total uncertainty (K) in the infilled analysis. Middle right:
1281 uncertainty (K) in the climatology component. Bottom left: uncertainty in the large-scale
1282 component (K). Bottom right: uncertainty in the local component (K).

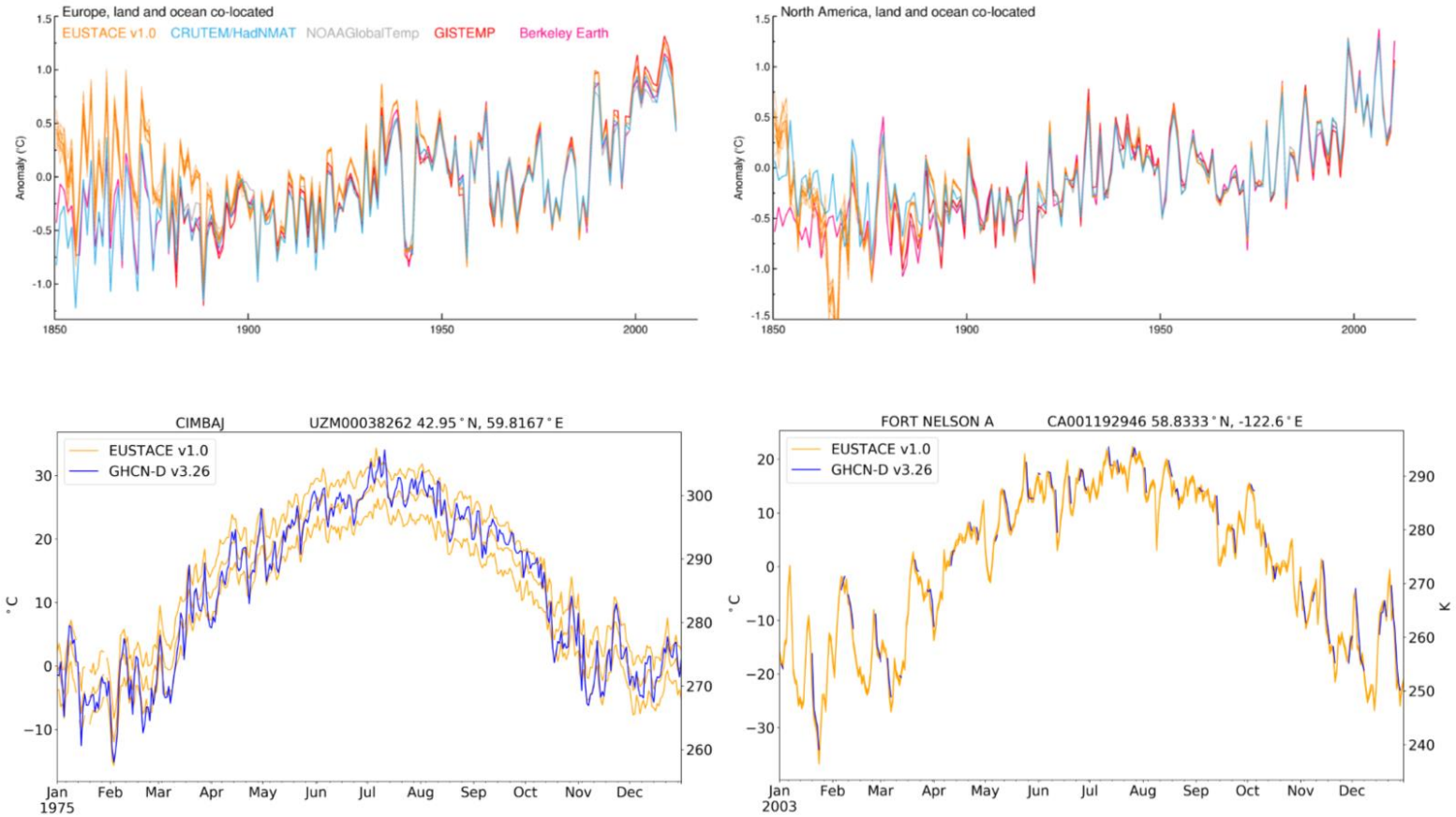


1283

1284 Figure 5. (Top) Annual regional average near surface air temperature anomaly (relative to 1961-1990) in a number of global surface

1285 temperature data sets, 1850-2015 (left: Europe; right: North America). Orange: EUSTACE global analysis v1.0; cyan: a blend of CRUTEM4 and

1286 HadNMAT2; grey: NOAAGlobalTemp; red: GISTEMP; pink: Berkley Earth. (Bottom) Daily near surface air temperature (K and $^{o}$C) over the

course of a year (left: Cimbaj, Uzbekistan in 1975; right: Fort Nelson, Canada in 2003). Orange: EUSTACE global analysis v1.0 (ensemble mean and range); royal blue: GHCN-D v3.26 station measurements.

1289

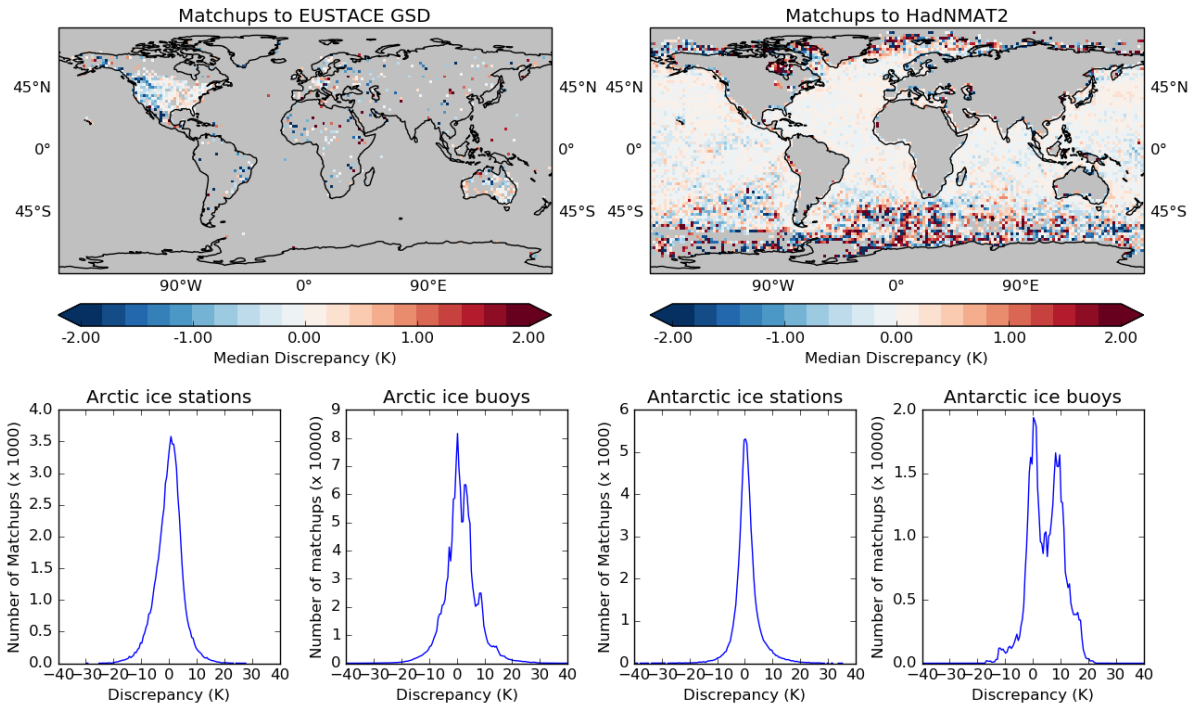


1290

1291 Figure 6. Validation of the EUSTACE global analysis v1.0, 1850-2015 against independent

1292 reference data. (Top left) median discrepancy (K) over land, compared to withheld station

1293 measurements. (Top right) median discrepancy (K) over ocean, compared to withheld ship

1294 measurements corrected to 2m. (Bottom row, left to right) discrepancy (K) between

1295 EUSTACE analysis and withheld reference data over ice-covered regions: Arctic land; Arctic

1296 sea ice; Antarctic land and Antarctic sea ice.

1297

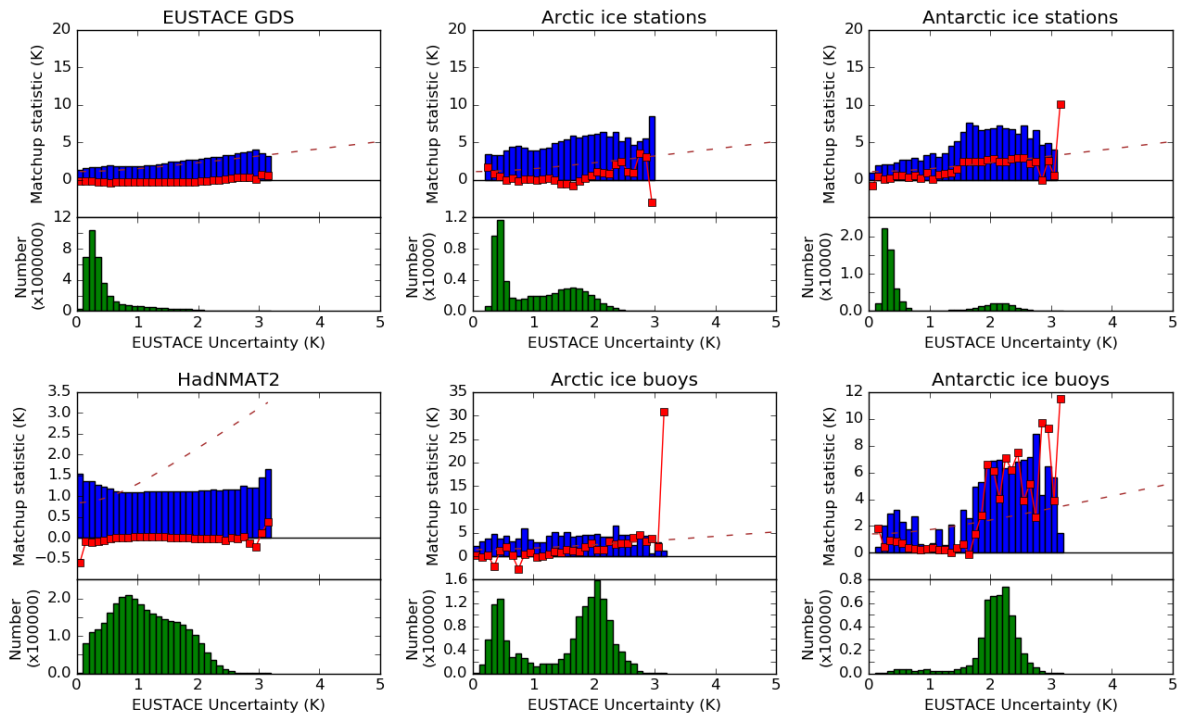


1298

1299 Figure 7. Validation of the uncertainty estimates for the EUSTACE global analysis v1.0, 1850-
1300 2015, against independent reference data. Top left: land; top middle: Arctic land ice; top
1301 right: Antarctic land ice; bottom left: ocean; bottom middle: Arctic sea ice; bottom right:
1302 Antarctic sea ice. Dashed line: modelled discrepancy; combined EUSTACE uncertainty and
1303 uncertainty in the validation data (K). Blue bars: robust standard deviation of discrepancies
1304 between the analysis and the validation data (K). Red line: median discrepancy (K). Green
1305 bars: number of matchups.